



Deposited via The University of Sheffield.

White Rose Research Online URL for this paper:

<https://eprints.whiterose.ac.uk/id/eprint/169828/>

Version: Accepted Version

---

**Article:**

Hunter, S.J. and Armes, S.P. (2020) Pickering emulsifiers based on block copolymer nanoparticles prepared by polymerization-induced self-assembly. *Langmuir*, 36 (51). pp. 15463-15484. ISSN: 0743-7463

<https://doi.org/10.1021/acs.langmuir.0c02595>

---

This document is the Accepted Manuscript version of a Published Work that appeared in final form in *Langmuir*, copyright © American Chemical Society after peer review and technical editing by the publisher. To access the final edited and published work see <https://doi.org/10.1021/acs.langmuir.0c02595>.

**Reuse**

Items deposited in White Rose Research Online are protected by copyright, with all rights reserved unless indicated otherwise. They may be downloaded and/or printed for private study, or other acts as permitted by national copyright laws. The publisher or other rights holders may allow further reproduction and re-use of the full text version. This is indicated by the licence information on the White Rose Research Online record for the item.

**Takedown**

If you consider content in White Rose Research Online to be in breach of UK law, please notify us by emailing [eprints@whiterose.ac.uk](mailto:eprints@whiterose.ac.uk) including the URL of the record and the reason for the withdrawal request.

# Pickering Emulsifiers Based on Block Copolymer Nanoparticles

## Prepared by Polymerization-Induced Self-Assembly

Saul J. Hunter and Steven P. Armes\*

<sup>†</sup>Department of Chemistry, Dainton Building, University of Sheffield,  
Brook Hill, Sheffield, South Yorkshire, S3 7HF, UK.

**ABSTRACT.** Block copolymer nanoparticles prepared *via* polymerisation-induced self-assembly (PISA) represent an emerging class of organic Pickering emulsifiers. Such nanoparticles are readily prepared by chain-extending a soluble homopolymer precursor using a carefully selected second monomer that forms an insoluble block in the chosen solvent. As the second block grows, it undergoes phase separation that drives *in situ* self-assembly to form sterically-stabilized nanoparticles. Conducting such PISA syntheses in aqueous solution leads to *hydrophilic* nanoparticles that enables the formation of oil-in-water emulsions. Alternatively, *hydrophobic* nanoparticles can be prepared in non-polar media (e.g. *n*-alkanes) which enables water-in-oil emulsions to be produced. In this review, the specific advantages of using PISA to prepare such bespoke Pickering emulsifiers are highlighted, which include fine control over particle size, morphology and surface wettability. This has enabled various fundamental scientific questions regarding Pickering emulsions to be addressed. Moreover, block copolymer nanoparticles can be used to prepare Pickering emulsions over various length scales, with mean droplet diameters ranging from millimeters to less than 200 nm.

\* Author to whom correspondence should be addressed ([s.p.arnes@sheffield.ac.uk](mailto:s.p.arnes@sheffield.ac.uk))

## INTRODUCTION

At the turn of the last century, Ramsden<sup>1</sup> and Pickering<sup>2</sup> independently discovered that various types of particles can stabilize emulsions. Over the past two decades, seminal studies by Binks and co-workers have led to a resurgence of interest in such Pickering emulsions.<sup>3-8</sup> This is because particulate emulsifiers offer numerous advantages over conventional surfactant or polymeric emulsifiers, including superior long-term emulsion stability and reduced foaming during homogenization.<sup>6</sup> Consequently, Pickering emulsions have been evaluated for various applications in food manufacture,<sup>9-11</sup> agrochemicals,<sup>12-15</sup> cosmetics<sup>16-17</sup> and pharmaceuticals.<sup>17-20</sup>

It is well-known that surfactants typically adsorb and desorb from interfaces on rapid timescales.<sup>21</sup> Unlike surfactants, colloidal particles that adsorb at oil/water or air/water interfaces are not necessarily amphiphilic.<sup>3, 5-7, 22-23</sup> Nevertheless, particles are often irreversibly adsorbed at an interface if they are of sufficient size and have appropriate surface wettability.<sup>24-26</sup> The driving force for particle adsorption is minimization of the interfacial area, which lowers the free energy of the system.<sup>6, 21</sup> The amount of energy,  $\Delta E$ , required to remove a spherical particle of radius  $r$  from the oil/water interface is given by equation 1:<sup>27</sup>

$$\Delta E = \pi r^2 \gamma_{ow} (1 \pm \cos \theta_w)^2 \quad (1)$$

where  $\gamma_{ow}$  is the oil/water interfacial tension and  $\theta_w$  is the three-phase contact angle. Figure 1 shows how the three-phase contact angle affects the detachment energy for a 20 nm particle adsorbed at the toluene/water interface.<sup>5</sup> The calculated energy of detachment is greatest for  $\theta_w = 90^\circ$  and falls rapidly either side of this value. The contact angle is directly related to the particle wettability, which dictates the type of emulsion that is formed.<sup>6</sup> More specifically, *hydrophilic* particles are preferentially wetted by the aqueous phase ( $\theta_w < 90^\circ$ ) and hence form oil-in-water (o/w) emulsions. In contrast, *hydrophobic* particles ( $\theta_w > 90^\circ$ ) give rise to water-in-oil (w/o) emulsions.<sup>5</sup> In principle, using a judicious combination of hydrophilic and

hydrophobic particles should enable the preparation of either water-in-oil-in-water (w/o/w) or oil-in-water-in-oil (o/w/o) Pickering double emulsions.<sup>28-29</sup>

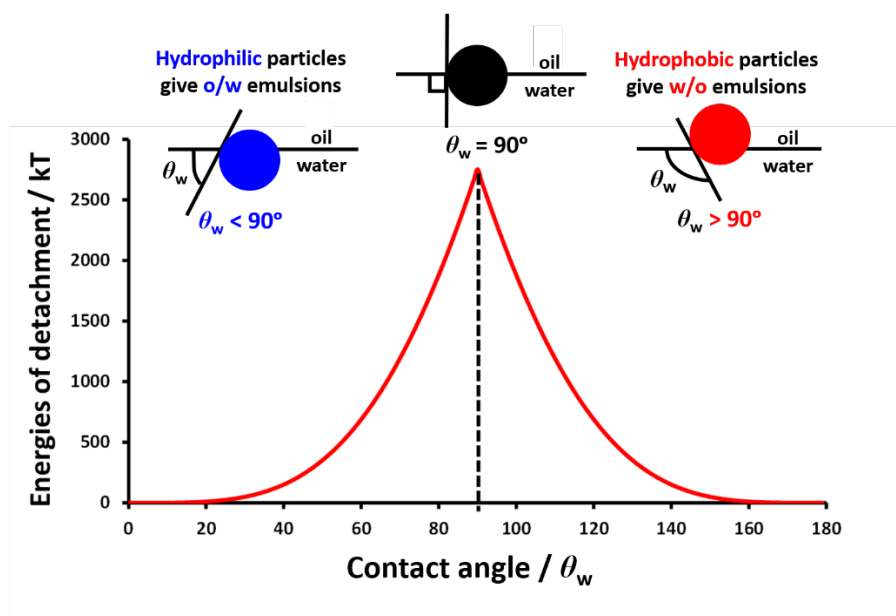


**Figure 1.** Spatial location of a spherical particle adsorbed at a planar oil-water interface for a contact angle  $\theta_w$  measured through the aqueous phase such that  $\theta_w$  is less than  $90^\circ$  (blue), equal to  $90^\circ$  (black) or greater than  $90^\circ$  (red). In general, hydrophilic particles ( $\theta_w < 90^\circ$ ) form oil-in-water (w/o) Pickering emulsions, whereas hydrophobic particles ( $\theta_w > 90^\circ$ ) give rise to water-in-oil (w/o) Pickering emulsions. The energy of detachment versus contact angle is shown for the specific case of a spherical nanoparticle of 10 nm radius adsorbed at a planar toluene-water interface for which  $\gamma_{ow} = 0.036 \text{ Nm}^{-1}$ .<sup>5-6</sup>

Many types of inorganic particles have been utilized as Pickering emulsifiers, including silica,<sup>3, 30</sup> titania,<sup>31-32</sup> magnetite,<sup>33</sup> and clay.<sup>3-4, 30-31, 33-37</sup> Similarly, various organic particles such as cellulose nanorods,<sup>38-41</sup> carbon black,<sup>42-43</sup> carbon nanotubes,<sup>44</sup> graphene oxide sheets<sup>45-46</sup> and aqueous polymer particles (e.g. latexes,<sup>22, 47-54</sup> microgels<sup>55-56</sup> and block copolymer nanoparticles<sup>57</sup>) have been evaluated in this context. Within the latter category, it is typically found that charge-stabilized latexes produce w/o emulsions whereas sterically-stabilized latexes usually form o/w emulsions, as depicted in Figure 2.<sup>22, 49</sup> Based on seminal studies by Binks and others, the use of *inorganic* particles to form Pickering emulsions is well understood.<sup>6, 21, 26, 35, 58-65</sup> In the prototypical case of silica, particle wettability can be tuned by partial alkylation of the silanol surface groups<sup>5</sup> or by adding either a cationic surfactant<sup>61, 66</sup> or electrolyte.<sup>3, 34</sup> However, such approaches tend to produce incipient flocculation in solution, which in turn leads to the formation of relatively thick multilayers of

adsorbed particles. In principle, polymer-based particles offer several advantages as Pickering emulsifiers. If they are designed to have appropriate surface wettability, no surface modification is required and adsorption at the oil-water interface leads to the formation of well-defined monolayers.<sup>3, 8, 22, 51, 57, 67-74</sup> Moreover, surface wettability can be readily tuned by selecting an appropriate steric stabilizer block<sup>73</sup>

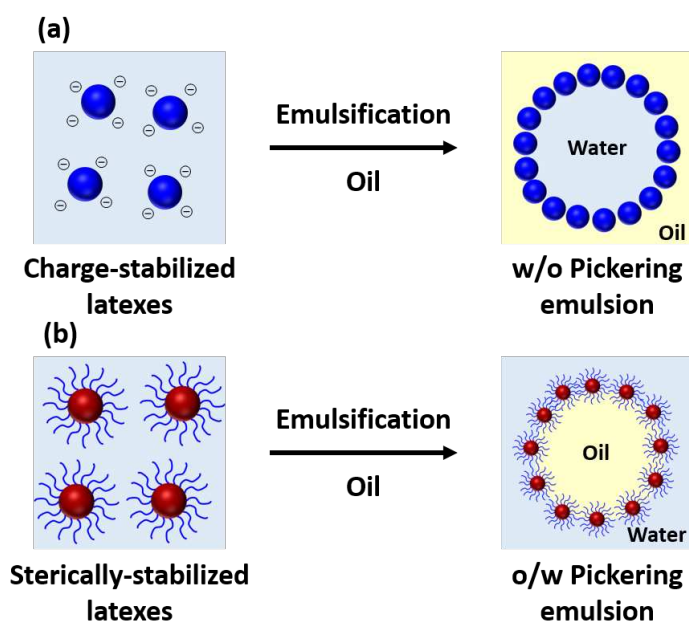


**Figure 2.** Schematic representation of the formation of (a) water-in-oil (w/o) Pickering emulsions using charge-stabilized latex particles or (b) oil-in-water (o/w) Pickering emulsions using sterically-stabilised latex particles via high-shear homogenization of an aqueous dispersion of latex particles with oil.

Velev and co-workers were the first to report using latex particles as Pickering emulsifiers.<sup>47</sup> In this case, the oil phase was 1-octanol and charge-stabilized polystyrene particles bearing either sulfate or amidine surface groups were utilized. Subsequently, Binks et al. used near-monodisperse polystyrene latex particles to stabilize w/o Pickering emulsions using cyclohexane as a model oil.<sup>22</sup> Weitz and co-workers developed colloidosomes using water-in-decalin Pickering emulsions stabilized by 0.7  $\mu\text{m}$  poly(methyl methacrylate) latex particles coated in a layer of poly(hydroxystearic acid).<sup>48</sup>

Subsequently, Binks, Armes and co-workers prepared a pH-sensitive polystyrene latex using a poly[2-(dimethylamino)ethyl methacrylate-*block*-methyl methacrylate] (PDMA-

PMMA) diblock copolymer as a steric stabilizer. The cationic character of the PDMA block could be adjusted by controlling the solution pH.<sup>49</sup> Such latex particles adsorbed onto *n*-hexadecane droplets when high shear homogenization was conducted at pH 8 to produce stable Pickering emulsions. However, stable emulsions could not be obtained at pH 3 because protonation of the PDMA block led to highly hydrophilic particles that were insufficiently wetted by the oil phase. Thus, such latexes simply exhibit pH-*dependent* Pickering emulsifier behavior,<sup>75</sup> as opposed to the pH-*responsive* behavior that was originally (and erroneously) reported.<sup>49-50</sup> In a related study, the thermoresponsive nature of the same PDMA-PMMA-stabilized polystyrene latex particles was explored.<sup>51</sup> Heating an o/w emulsion stabilized by such particles up to 70 °C (i.e. above the cloud point of the hydrophilic PDMA block) led to significant droplet coalescence. Moreover, w/o emulsions were obtained if the same aqueous latex and oil were separately heated to 70 °C prior to emulsification. The relatively hydrophobic nature of the flocculated particles under such conditions accounts for this phase inversion.<sup>51</sup>

In related work, Fujii et al. prepared lightly cross-linked poly(4-vinylpyridine)/silica nanocomposite particles for use as *stimulus-responsive* Pickering emulsifiers.<sup>76-77</sup> Such particles stabilized Pickering emulsions at pH 8-9, but addition of acid caused rapid demulsification. This is because protonation of the 4-vinylpyridine units at low pH induces particle swelling: lateral repulsion between the resulting highly swollen cationic microgel-like particles leads to their desorption from the oil-water interface. Similarly, pH-responsive Pickering emulsifiers based on polymer latexes also been reported. For example, Morse and co-workers prepared lightly cross-linked latexes composed of either poly(2-(*tert*-butylamino)ethyl methacrylate) or poly(2-(diethylamino)ethyl methacrylate).<sup>78-79</sup> Such sterically-stabilized latexes act as effective Pickering emulsifiers at pH 10 but acidification resulted in rapid demulsification owing to a latex-to-microgel transition. In principle, such

Pickering emulsifiers can be reused by raising the solution pH to its original value. In practice, the progressive build-up of background salt leads to a gradual reduction in microgel swelling, which effectively limits the number of pH cycles.<sup>79</sup>

Another class of stimulus-responsive Pickering emulsifier is the poly(*N*-isopropylacrylamide) (PNIPAM)-based microgels originally reported by Ngai et al. and further developed by Richtering and co-workers.<sup>55-56, 80-81</sup> PNIPAM homopolymer exhibits a lower critical solution temperature (LCST) at around 32 °C.<sup>82</sup> Thus, aqueous dispersion copolymerization of NIPAM with bisacrylamide cross-linker using persulfate as a free radical initiator at 70 °C affords a charge-stabilized latex and the resulting lightly cross-linked particles exhibit a latex-to-microgel transition on cooling below this temperature.<sup>83-85</sup> Moreover, pH-responsive PNIPAM-based microgels can be prepared by introducing methacrylic acid (MAA) as a comonomer. Ngai et al. reported the first example of a dual temperature- and pH-responsive Pickering emulsifier.<sup>55, 80</sup> The incorporation of MAA units within the PNIPAM-based particles led to microgel swelling on raising the solution pH. Thus, o/w emulsions stabilized by such P(NIPAM-*co*-MAA) microgels are stable at 25 °C and pH 9.4, but become unstable at 60 °C on lowering the pH to 6.1.<sup>55, 80</sup> This is because the adsorbed microgels shrink at the oil-water interface, thus leading to a reduction in surface coverage and hence droplet coalescence.<sup>86</sup> In follow-up studies, Richtering and co-workers have postulated that the viscoelastic behavior of the microgel-coated interface determines the emulsion stability.<sup>56, 81, 87-90</sup>

The invention of living anionic polymerization by Szwarc et al.<sup>91-92</sup> in the 1950s ultimately enabled the rational design of various examples of amphiphilic diblock copolymers such as poly(ethylene oxide)-polystyrene or poly(acrylic acid)-polystyrene. It is well-established by Eisenberg et al.<sup>93-95</sup> and others<sup>96</sup> that such amphiphilic diblock copolymers undergo self-assembly in aqueous solution to form spherical, worm-like or

vesicular nano-objects.<sup>93-94, 96-98</sup> Such self-assembly is enthalpically driven and depends on both  $\chi$  and  $N$ , where  $\chi$  is the Flory-Huggins interaction parameter and  $N$  is the overall degree of polymerization of the copolymer chains.<sup>97</sup> However, traditional post-polymerization processing routes invariably involve organic co-solvents such as DMF or THF, gradual addition of water over prolonged time scales and relatively low copolymer concentrations (< 1.0% w/w), which unfortunately preclude many potential commercial applications.

Fortunately, the development of controlled radical polymerization techniques<sup>99-101</sup> such as reversible addition-fragmentation chain transfer (RAFT) polymerization<sup>102-105</sup> has enabled the efficient synthesis of block copolymer nano-objects *via* polymerization-induced self-assembly (PISA).<sup>106-115</sup> Importantly, RAFT polymerization is exceptionally tolerant of monomer functionality, which enables the rational design of nano-objects bearing hydroxyl, amine or carboxylic acid groups. Moreover, such PISA syntheses can be conducted at relatively high copolymer concentrations (up to 50% w/w).<sup>116-117</sup> In a typical protocol, a soluble homopolymer is chain-extended using a second monomer in a suitable solvent such that the growing second block gradually becomes insoluble, which drives *in situ* self-assembly to form diblock copolymer nanoparticles, as depicted in Figure 3. Depending on the solubility of the second monomer in the continuous phase, the synthesis of the insoluble second block involves either dispersion or emulsion polymerization.<sup>108, 118-134</sup> Systematic variation of the relative volume fractions of the two blocks provides control over the copolymer morphology.<sup>116, 135-136</sup> Over the past decade or so, the generic nature of PISA has been demonstrated for a wide range of vinyl monomers in various solvents including water,<sup>132, 137-143</sup> polar solvents (e.g. ethanol or methanol),<sup>144-157</sup> non-polar solvents (e.g. *n*-alkanes),<sup>110, 158-163</sup> ionic liquids,<sup>164</sup> silicone oil<sup>165-166</sup> and supercritical CO<sub>2</sub>.<sup>167-170</sup> Typically, pseudo-phase diagrams are constructed to enable the reproducible targeting of morphologies for a given PISA formulation.<sup>140</sup> The basic design rules for the preparation of spheres,<sup>140, 158</sup>

worms,<sup>171-175</sup> vesicles,<sup>176-179</sup> framboidal vesicles,<sup>72, 137, 180-181</sup> and lamellae<sup>182-184</sup> are now well-established. In many cases, the final copolymer morphology is dictated primarily by the relative volume fractions of the two blocks, as indicated by the geometric packing parameter introduced by Israelachvili and co-workers to account for surfactant self-assembly.<sup>185</sup> For example, spheres are produced when using a relatively long soluble stabilizer block and/or working at relatively low copolymer concentrations,<sup>140, 158</sup> while vesicles can be obtained when targeting highly asymmetric diblock compositions (i.e. relatively long insoluble blocks) at higher copolymer concentrations.<sup>137, 145</sup> It is also well-established that worm-like particles typically occupy relatively narrow phase space between that of spheres and vesicles,<sup>162, 171-172</sup> framboidal vesicles can be produced from ABC triblock copolymers in which the B and C blocks are both insoluble and enthalpically incompatible,<sup>72, 186</sup> and targeting stiff, inflexible insoluble blocks favors lamellae formation.<sup>183-184</sup>

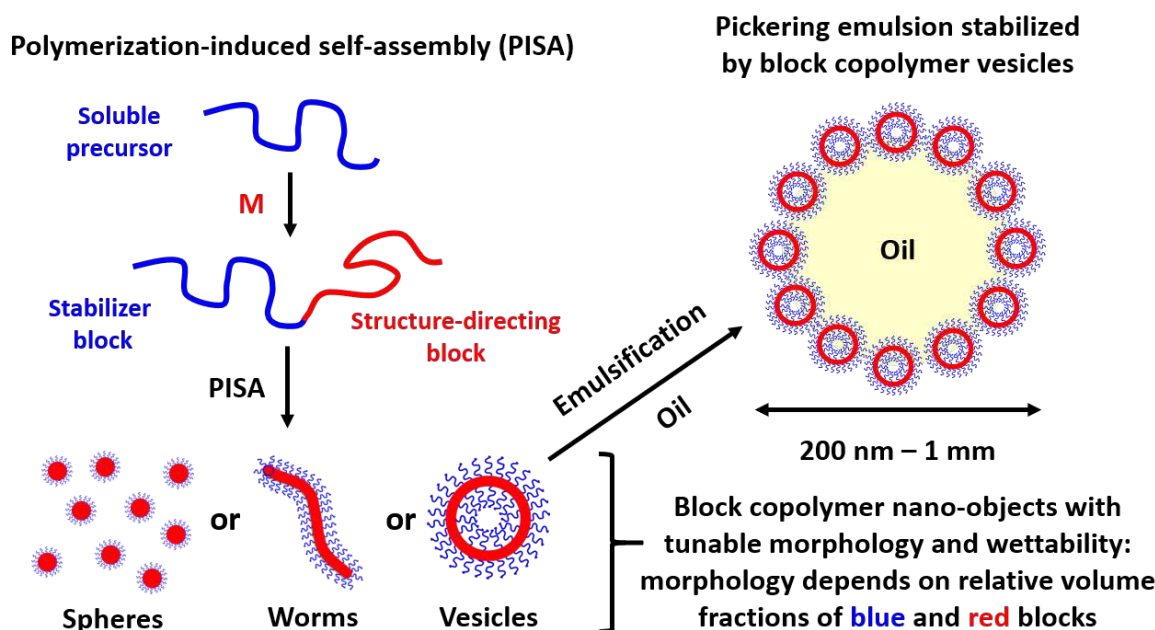


**Figure 3.** Schematic representation of polymerization-induced self-assembly (PISA), whereby a soluble blue precursor block is chain-extended using a suitable vinyl monomer to produce a red insoluble structure-directing block. Depending on the relative volume fractions of the blue and red blocks, *in situ* self-assembly produces either spheres, worms or vesicles. PISA can be conducted in either water or various oils. In the case of aqueous PISA, addition of a suitable oil followed by emulsification via high shear homogenization leads to the formation of Pickering emulsions, as illustrated above for the case of vesicles.<sup>187</sup>

Recently, we have exploited PISA to design new block copolymer nano-objects for use as bespoke Pickering emulsifiers.<sup>71-74, 117, 187-195</sup> More specifically, PISA enables the copolymer morphology and surface chemistry to be tuned by judicious selection of the soluble stabilizer and insoluble structure-directing blocks. Such syntheses can be conducted in either water or in *n*-alkanes to afford either *hydrophilic* or *hydrophobic* sterically-stabilized nanoparticles, respectively. Such nanoparticles can be used to prepare oil-in-water,<sup>117, 187-188</sup> water-in-oil<sup>71, 189</sup> and multiple emulsions.<sup>73, 191</sup> In particular, the versatility offered by PISA enables interesting scientific questions to be addressed in the context of Pickering emulsions. Do such linear block copolymer nanoparticles survive high-shear homogenization or is their covalent stabilization required? Can we readily distinguish between these two scenarios? Can vesicles be used to stabilize Pickering emulsions? Do worms offer any advantages over spheres? Does refractive index matching enable highly transparent Pickering emulsions to be prepared? Can spheres be made sufficiently small (and stable) to enable the preparation of Pickering nanoemulsions? What is the effect of introducing minimal nanoparticle surface charge on Pickering emulsion formation and stability? Such research topics are discussed in the remaining sections of this review article.

## **EFFECT OF COPOLYMER MORPHOLOGY ON PICKERING EMULSIFIER PERFORMANCE**

Thompson et al. reported the first example of polymer-based Pickering emulsifiers prepared via PISA.<sup>187</sup> Linear poly(glycerol monomethacrylate)-poly(2-hydroxypropyl methacrylate) PGMA<sub>45</sub>-PHPMA<sub>200</sub> diblock copolymer vesicles were prepared at 10% w/w solids using a RAFT aqueous dispersion polymerization formulation (see Figure 4a). Such linear (non-cross-linked) vesicles did not survive the high-shear homogenization conditions required for emulsification with *n*-dodecane. Instead, *in situ* dissociation occurred and the resulting oil droplets became stabilized by individual amphiphilic PGMA<sub>45</sub>-PHPMA<sub>200</sub>

chains. This problem was confirmed using two characterization techniques. Firstly, the volume-average oil droplet diameter determined by laser diffraction proved to be independent of the copolymer concentration (see Figure 4b), whereas a strong concentration dependence is invariably observed for Pickering emulsions.<sup>58, 196</sup>

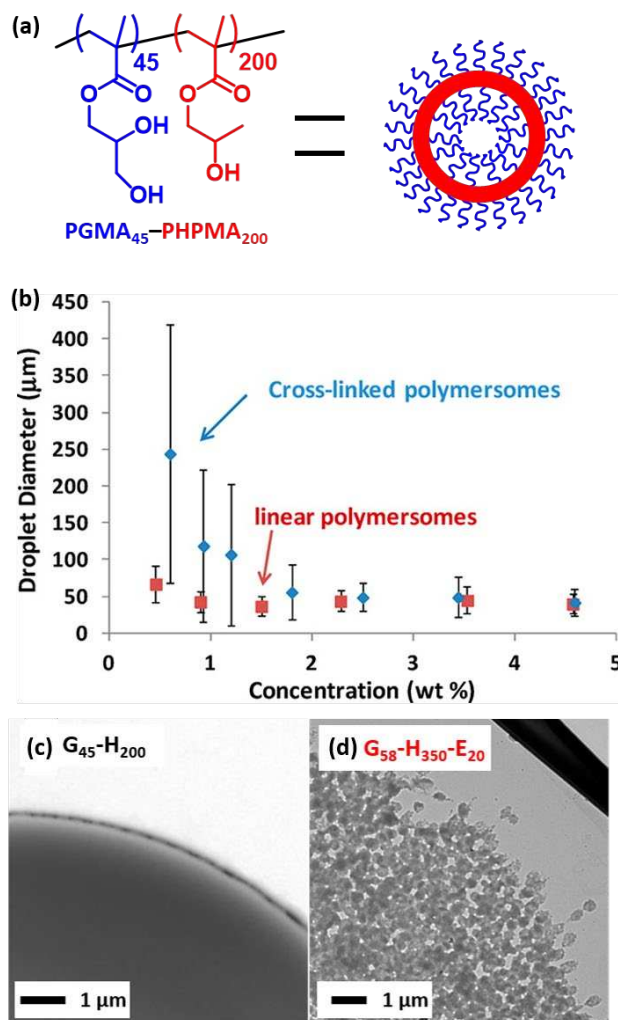


**Figure 4.** (a) Chemical structure of linear PGMA<sub>45</sub>-PPHMA<sub>200</sub> vesicles. (b) Volume-average droplet diameter (obtained by laser diffraction) vs. copolymer concentration for both linear PGMA<sub>45</sub>-PPHMA<sub>200</sub> and cross-linked PGMA<sub>58</sub>-PPHMA<sub>350</sub>-PEGDMA<sub>20</sub> vesicles. TEM images recorded for an individual dried cross-linked colloidosome prepared using (c) linear PGMA<sub>45</sub>-PPHMA<sub>200</sub> vesicles and (d) cross-linked PGMA<sub>58</sub>-PPHMA<sub>350</sub>-PEGDMA<sub>20</sub> vesicles. Reproduced from ref. 187 (Copyright 2012 American Chemical Society).

Secondly, TEM studies of the dried oil droplets indicated a smooth, featureless morphology with no evidence for the original vesicles, see Figure 4c. This study highlighted the importance of verifying the formation of genuine Pickering emulsions when using block copolymer nanoparticles. *In situ* vesicle dissociation was attributed to the weakly

hydrophobic nature of the membrane-forming PHPMA block.<sup>197-198</sup> In view of this problem, ethylene glycol dimethacrylate (EGDMA) was added as a third comonomer to form cross-linked vesicles, which proved to be stable when subjected to high-shear homogenization.<sup>187</sup> In this case, the expected upturn in oil droplet diameter was observed as the vesicle concentration was lowered. Furthermore, TEM studies revealed the presence of intact vesicles at the oil/water interface (see Figure 4c). Such vesicle-stabilized Pickering emulsions could be covalently-stabilized by dissolving a tolylene-2,4-diisocyanate-terminated poly(propylene glycol) diisocyanate cross-linker (PPG-TDI) in the oil phase prior to homogenization, leading to the formation of so-called colloidosomes.<sup>48, 187, 199</sup>

Turbidimetry experiments indicated that most of the vesicles were not adsorbed at the oil/water interface and instead remained within the continuous aqueous phase. As the copolymer concentration used to prepare such Pickering emulsions was reduced from 2.5% to 0.6% w/w, the vesicle adsorption efficiency increased from 57 to 78% w/w. The relatively weak affinity of the vesicles for the oil/water interface is presumably related to their aqueous cores, which necessarily lowers the Hamaker constant and hence reduces the enthalpy of adsorption.

Subsequently, Thompson and co-workers reported that linear PGMA-PHPMA spheres and worms also underwent *in situ* dissociation to form soluble copolymer chains during high shear homogenization.<sup>188</sup> However, laser diffraction studies confirmed that this problem could be circumvented by either covalent stabilization using EGDMA cross-linker or by addition of a sufficiently hydrophobic third block such as poly(benzyl methacrylate) (PBzMA), see Figure 5. Using the former strategy, PGMA<sub>100</sub>-PHPMA<sub>200</sub>-PEGDMA<sub>20</sub> spheres and PGMA<sub>45</sub>-PHPMA<sub>100</sub>-PEGDMA<sub>10</sub> worms were prepared via PISA and their performance as putative Pickering emulsifiers for the stabilization of *n*-dodecane-in-water emulsions was compared.<sup>188</sup> It is well-established that worms are formed during PISA via 1D stochastic

fusion of multiple spheres.<sup>139-140, 200</sup> This is important, because it means that the mean worm thickness is directly related to the dimensions of the initial spheres. Moreover, given that both types of nanoparticles utilized a hydroxyl-functional PGMA block as a steric stabilizer (see Figure 4a), essentially identical surface wettabilities can be assumed. Thompson and co-workers<sup>188</sup> argued that, for sufficiently anisotropic worms, their specific surface area,  $A_w$ , can be estimated using the relation  $A_w \sim 2/\rho R$ , where  $\rho$  is the particle density and  $R$  is the mean worm cross-sectional radius. In contrast, prior to their 1D fusion to form worms, the spheres have a specific surface area,  $A_s$ , given by  $A_s = 3/\rho r$ , where  $r$  is the mean sphere radius and, to a reasonable approximation,  $r \sim R$ . Therefore, the reduction in specific surface area ( $A_w/A_s$ ) that occurs during the 1D fusion of multiple spheres to form a single worm is only around 33%, whereas the energy of attachment of a sufficiently anisotropic worm ( $L/2R > 20$ ) composed of  $x$  spheres is estimated to be at least  $x$  times higher than the individual spherical nanoparticles. In summary, highly anisotropic diblock copolymer worms are expected to adsorb at an oil-water interface much more strongly than the corresponding precursor diblock copolymer spheres, while retaining a relatively high specific surface area. Turbidimetry studies conducted on the lower aqueous phase formed after emulsion creaming indicated relatively high adsorption efficiencies ( $\sim 90\%$ ) for both spheres and worms. More importantly, the worms produced significantly finer *n*-dodecane droplets than the spheres. This was attributed to the highly anisotropic nature of the former nanoparticles, which allows the droplet surface to become sufficiently coated to prevent coalescence at approximately half the surface coverage. Similar observations were made by Vermant and co-workers, who found that Pickering emulsions prepared using polystyrene rods were more stable relative to their spherical precursors.<sup>201-202</sup> Such experiments account for the excellent Pickering emulsion performance observed for highly anisotropic cellulose nanofibers, for which no spherical counterparts

exist.<sup>38</sup> More broadly, various groups have reported that model anisotropic particles differ fundamentally in their interfacial adsorption behavior compared to isotropic particles.<sup>54, 203-205</sup>

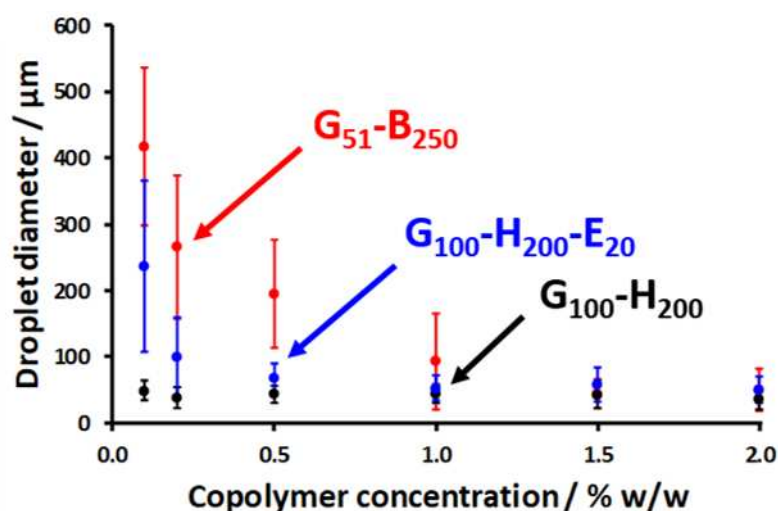


**Figure 5.** Volume-average droplet diameter versus copolymer concentration obtained by laser diffraction analysis of *n*-dodecane-in-water emulsions prepared using linear (red) PGMA<sub>51</sub>-PBzMA<sub>250</sub>, (black) PGMA<sub>100</sub>-PHPMA<sub>200</sub> spheres and (blue) cross-linked PGMA<sub>100</sub>-PHPMA<sub>200</sub>-PEGDMA<sub>20</sub> spheres. Error bars represent the standard deviation for each droplet diameter, rather than the experimental error. Reproduced from ref. 188 (Copyright 2014 Royal Society of Chemistry).

Thompson et al. also directly compared the Pickering emulsifier performance of linear hydrophobic poly(lauryl methacrylate)-poly(benzyl methacrylate) (PLMA-PBzMA) worms and spheres prepared in *n*-dodecane.<sup>189</sup> For this PISA formulation, the worms are thermoresponsive and can be transformed into spheres when heated to 150 °C owing to surface plasticization of the core-forming PBzMA chains.<sup>159</sup> Moreover, this morphological transition is effectively irreversible if it is conducted at sufficiently low copolymer concentration (e.g.,  $\leq 1.0\%$  w/w).<sup>159</sup> Thus, the Pickering performance of highly anisotropic PLMA<sub>16</sub>-PBzMA<sub>37</sub> worms for the stabilization of w/o emulsions could be compared to that of *chemically identical* spheres for the first time. Again, significantly smaller mean droplet diameters ( $D$ ) were observed for the worms when working above a certain critical copolymer mass ( $m_p$ ). Furthermore, the fractional droplet surface coverage,  $C$ , differed markedly for worms and spheres (see Figure 6). As expected, spherical nanoparticles exhibited a constant surface coverage with copolymer concentration. In contrast, higher surface coverages were

observed for worms at higher copolymer concentration. The isotropic nature of spheres means that maximum packing requires six inter-particle contacts with nearest neighbors, whereas worms can form a loose packing at low concentration and a more densely-packed layer at relatively high concentration. Similar observations have been made for anisotropic cellulose nanofibers.<sup>38-39</sup> Relatively short fibers formed a densely-packed layer at the oil/water interface, whereas longer fibers led to lower surface coverages with a more open 2D network.<sup>39</sup> Small-angle X-ray scattering (SAXS) studies conducted on a worm-stabilized Pickering emulsion indicated that the mean thickness of the worm layer surrounding the water droplets is comparable to the worm cross-sectional diameter. This indicates monolayer coverage rather than multilayer formation. Finally, the thermoresponsive behavior of PLMA<sub>16</sub>-PBzMA<sub>37</sub> worms was exploited to induce demulsification. Heating the w/o Pickering emulsion up to 95 °C induces a worm-to-sphere transition, with concomitant droplet coalescence being observed owing to copolymer desorption from the oil/water interface.

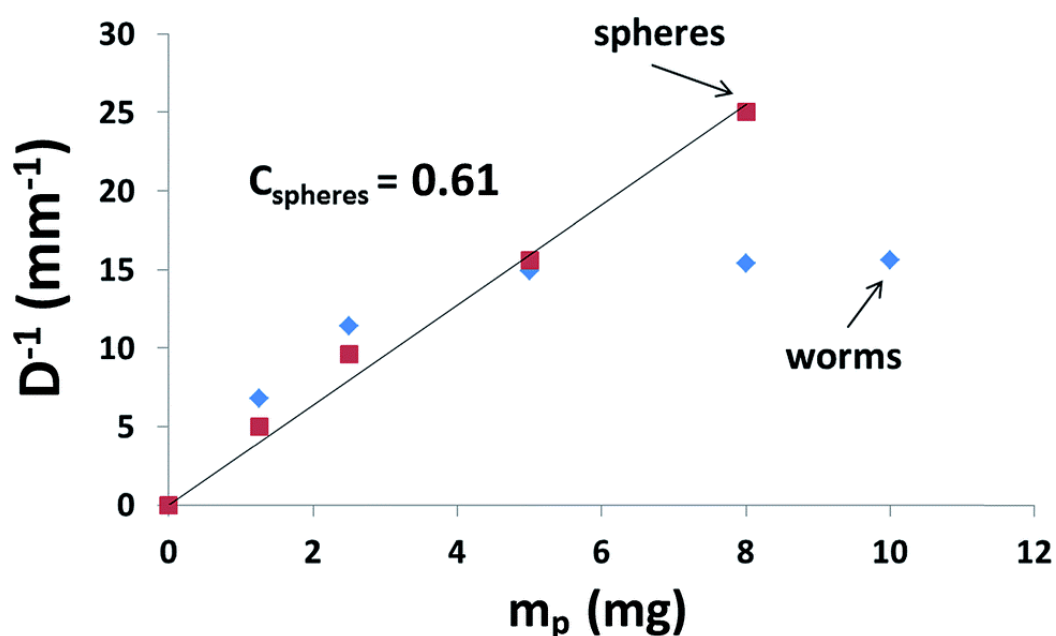


**Figure 6.** Effect of varying the copolymer particle mass  $m_p$  on the mean droplet diameter  $D$  for two series of water-in-*n*-dodecane emulsions stabilized using PLMA<sub>16</sub>-PBzMA<sub>37</sub> spheres (red circles) and PLMA<sub>16</sub>-PBzMA<sub>37</sub> worms (blue squares). Note the deviation from linearity for the latter particles. Reproduced from ref. 189 (Copyright 2015 Royal Society of Chemistry).

Xue and co-workers compared the stability of diblock copolymer worms and spheres when such nano-objects were subjected to high-shear homogenization.<sup>206</sup> To prepare such diblock copolymer nanoparticles, poly(*N*-(2-methacryloyloxy)ethyl pyrrolidone) (PNMP<sub>53</sub>) was chain-extended by RAFT polymerization of 2-perfluorooctylethyl methacrylate (FMA) in chloroform. The resulting PNMP<sub>53</sub>-PFMA<sub>x</sub> block copolymers were then self-assembled to form either spheres ( $x = 5$ ) or worms ( $x = 10$ ) in water by traditional post-polymerization processing via a solvent switch. Oil-in-water Pickering emulsions were prepared by high shear homogenization of aqueous dispersions of such nanoparticles with *n*-dodecane. TEM and laser diffraction studies confirmed that both types of nanoparticles survived emulsification, presumably owing to the highly hydrophobic nature of the PFMA core-forming block. This study used the twisted intramolecular charge transfer state (TICT) of Nile Red to distinguish between the fluorescence of this dye dissolved in *n*-dodecane droplets and that within the nanoparticle cores. More specifically, the excitation and emission wavelengths for Nile Red dissolved in *n*-dodecane are 490-520 nm and 530-570 nm respectively, whereas these bands are red-shifted to 576 nm and 621 nm respectively for the dye-loaded nanoparticles.<sup>206</sup> Thus, if Nile Red was solubilized within the nanoparticles prior to emulsification, excitation at 576 nm led to significantly greater fluorescence intensity than that observed for the oil droplets, indicating that the nanoparticles were adsorbed at the oil/water interface in the form of Pickering emulsions.

The effect of varying the shear rate on the fluorescence intensity of the dye dissolved in the oil droplets ( $I_{oil}$ ) relative to that for the dye-loaded PNMP<sub>53</sub>-PFMA<sub>5</sub> spheres ( $I_{layer}$ ) was also examined. As expected, greater shear rates led to higher  $I_{oil}/I_{layer}$  ratios (see Figure 7).<sup>206</sup> For example, dye fluorescence originating from the oil droplets dominates at 24,000 rpm, indicating that such conditions cause *in situ* nanoparticle dissociation, leading to emulsion stabilization by the individual amphiphilic PNMP<sub>53</sub>-PFMA<sub>5</sub> diblock copolymer chains. A

similar experiment was conducted using the PNMP<sub>53</sub>-PFMA<sub>10</sub> worms. In this case, at least some of the worms remained intact at 24,000 rpm. The authors of this study attributed this observation to the worms being less susceptible to degradation under shear than the spheres. However, it seems much more likely that the greater stability of the worms is simply the result of the higher DP of the hydrophobic PFMA block that is required to form such nano-objects.<sup>188</sup> Although these PNMP<sub>53</sub>-PFMA<sub>x</sub> spheres and worms were prepared by traditional post-polymerization processing, this study is clearly consistent with the observation of *in situ* nanoparticle dissociation reported when using linear diblock copolymer nano-objects prepared via PISA. Moreover, it confirms that such dissociation can occur even when using highly hydrophobic perfluorinated structure-directing blocks, although the mean DPs of such chains are admittedly rather low.

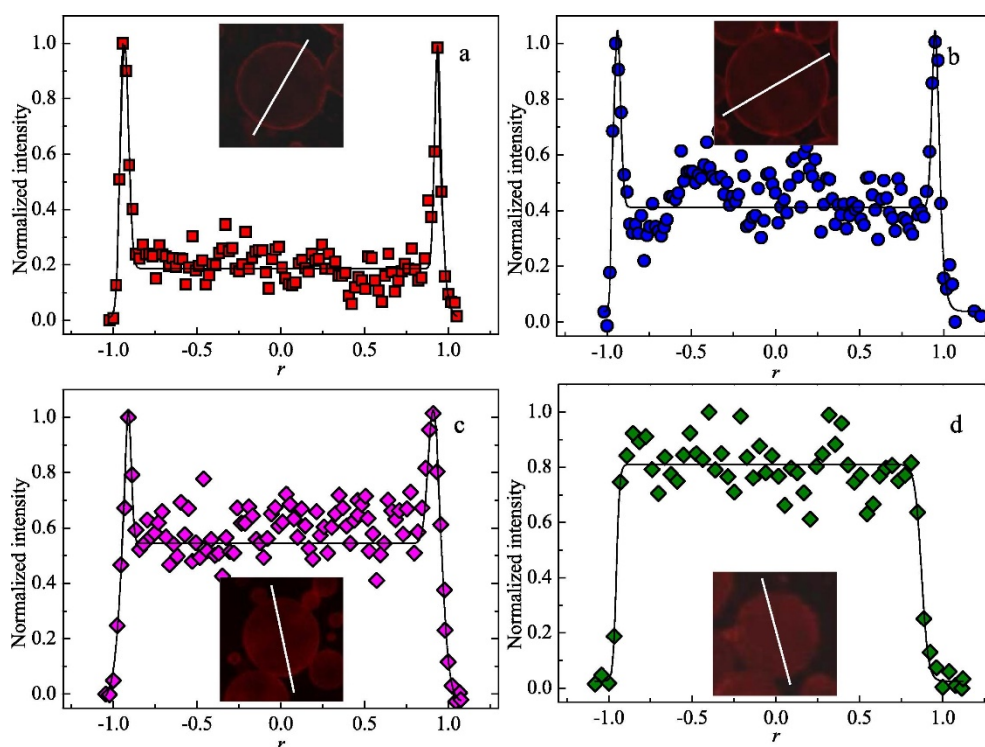


**Figure 7.** Fluorescence data recorded as a function of distance  $r$  (with data fits using both Gaussian and Boltzmann methods) obtained for an  $n$ -dodecane-in-water Pickering emulsion prepared at an oil volume fraction of 0.50 using 0.50% w/w PNMP<sub>53</sub>-PFMA<sub>5</sub> via high shear homogenization at (a) 6,000 rpm, (b) 12,000 rpm, (c) 18,000 rpm or (d) 24,000 rpm, respectively. In each case, the inset confocal microscopy image shows the individual emulsion droplet and the white line indicates the cross-sectional diameter through which the fluorescence intensity is calculated as a function of  $r$ . Reproduced from ref. 206 (Copyright 2020 Elsevier).

Recently, we reported the effect of nanoparticle anisotropy on the stability of an o/w Pickering emulsion in the presence of a non-ionic surfactant.<sup>194</sup> RAFT aqueous dispersion polymerization was used to prepare epoxy-functional PGMA<sub>48</sub>-P(HPMA<sub>90</sub>-*stat*-GlyMA<sub>15</sub>) worms (where GlyMA denotes glycidyl methacrylate). The thermoresponsive nature of such linear precursor nanoparticles was exploited to produce either relatively long or relatively short cross-linked worms of essentially the same copolymer composition.<sup>207</sup> More specifically, 3-aminopropyltriethoxysilane (APTES) was utilized in a post-polymerization crosslinking protocol developed by Lovett et al.<sup>208</sup> The primary amine group in this reagent reacts with the epoxy groups on the GlyMA units while its siloxy groups react with the secondary alcohol groups on the HPMA units to confer covalent stabilization. Either relatively long or relatively short cross-linked worms were prepared to stabilize *n*-dodecane-in-water Pickering emulsions, with a fluorescent label being introduced by reacting rhodamine B piperazine with a minor fraction of the epoxy groups on the GlyMA residues prior to APTES addition. This enabled fluorescence microscopy to be used to monitor the precise location of the worms before and after addition of the non-ionic surfactant to each Pickering emulsion (see Figure 8). A much higher surfactant concentration was required to displace long worms from the oil/water interface compared to the short worms. This is because the former nanoparticles are much more strongly adsorbed than the latter.<sup>188-189</sup>

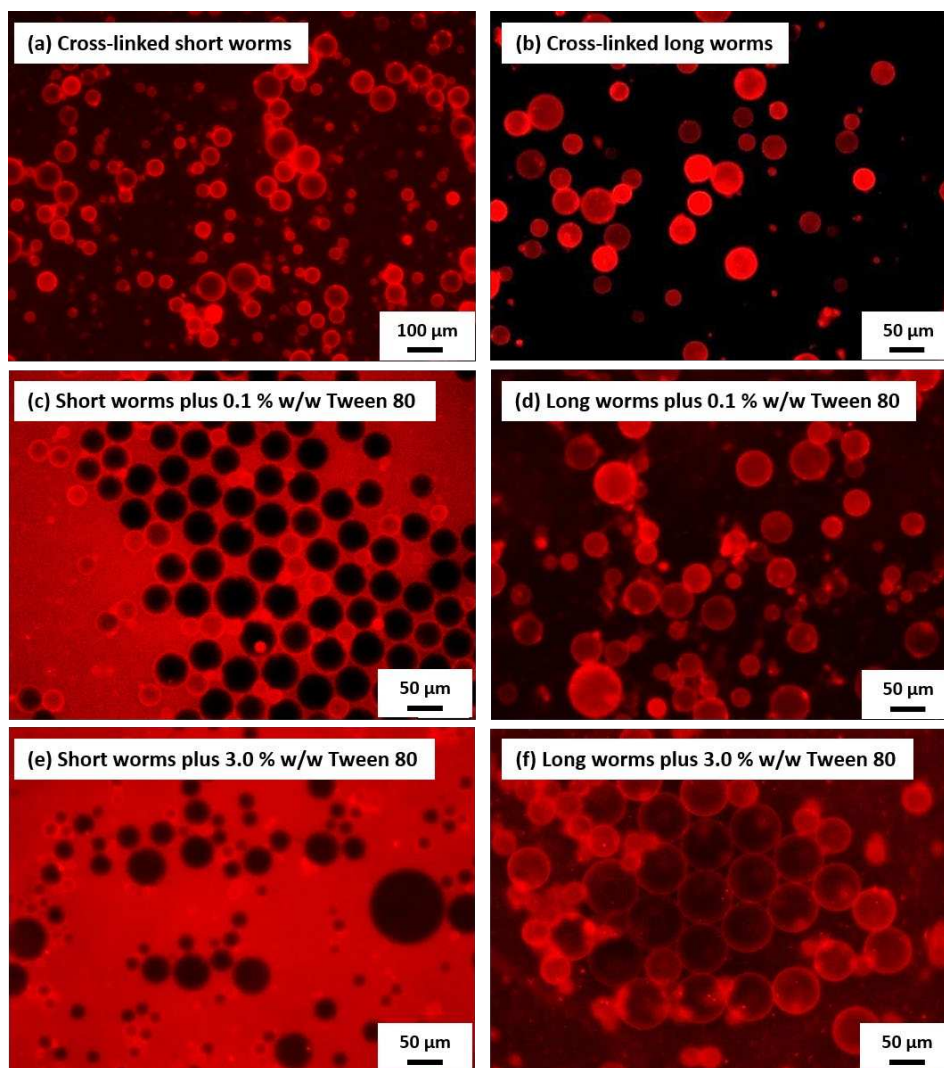


**Figure 8.** Fluorescence microscopy images obtained for emulsions prepared by high shear homogenization of 0.25% w/w aqueous PGMA<sub>48</sub>-P(HPMA<sub>90</sub>-*stat*-GlyMA<sub>15</sub>) copolymer dispersions with 50 vol % *n*-dodecane at 13,500 rpm for 2 min, before and after addition of either 0.1% or 3.0% w/w non-ionic surfactant (Tween 80). (a) Pickering emulsion stabilized using short PGMA<sub>48</sub>-P(HPMA<sub>90</sub>-*stat*-GlyMA<sub>15</sub>) cross-linked worms (b) Pickering emulsion stabilized using long PGMA<sub>48</sub>-P(HPMA<sub>90</sub>-*stat*-GlyMA<sub>15</sub>) cross-linked worms. (c) Surfactant-stabilized emulsion obtained after addition of 0.1% w/w Tween 80, which displaces the short worms initially adsorbed at the oil/water interface. (d) Pickering emulsion obtained after addition of 0.1% w/w Tween 80, which *cannot* displace the long worms initially adsorbed at the oil/water interface. (e) Surfactant-stabilized emulsion obtained after addition of 3.0% w/w Tween 80, which displaces the short worms adsorbed at the oil/water interface. (f) Mixed emulsion obtained after addition of 3.0% w/w Tween 80, which *partially* displaces the long worms adsorbed at the oil/water interface. Reproduced from ref. 194 (Copyright 2018 American Chemical Society).

Zhang and co-workers utilized cross-linked triblock copolymer worms to prepare high internal phase Pickering emulsions (HIPEs) in which the volume fraction of the dispersed phase exceeded 0.74.<sup>209</sup> Such worms were first prepared *via* RAFT dispersion polymerization of BzMA in ethanol using a poly(2-(dimethylamino)ethyl methacrylate) (PDMA) precursor. These linear PDMA<sub>37</sub>-PBzMA<sub>96</sub> worms were subsequently cross-linked via chain extension using EGDMA. After transferring the covalently-stabilized PDMA<sub>37</sub>-PBzMA<sub>96</sub>-PEGDMA<sub>9</sub>

worms into water, the resulting dispersion was subjected to high shear homogenization with varying amounts of cyclohexane. Highly viscous HIPEs possessing an internal phase ranging from 0.77 to 0.84 exhibited good long-term stability. Furthermore, a remarkably low copolymer concentration (0.3%) was sufficient to stabilize a HIPE prepared at an oil volume fraction of 0.77. This remarkable observation was attributed to the dense gel network formed by the highly anisotropic worms. To prepare porous monoliths, either silica or  $\text{Fe}_3\text{O}_4$  nanoparticles were added to the aqueous phase prior to homogenization to act as a co-stabilizer. After freeze-drying for 12 h, the 3D hierarchical structure survived in the form of a free-standing porous monolith. In the case of the  $\text{Fe}_3\text{O}_4$  nanoparticles, such ultralight hybrid materials proved to be responsive to an applied magnetic field.<sup>209</sup>

Chambon and co-workers reported that chain extension of PGMA-PPMA precursor vesicles using a water-immiscible monomer such as BzMA or MMA resulted in the formation of framboidal (raspberry-like) triblock copolymer vesicles *via* seeded RAFT aqueous emulsion polymerization.<sup>186</sup> Subsequently, a series of  $\text{PGMA}_{63}\text{-PHPMA}_{350}\text{-PBzMA}_z$  framboidal vesicles were evaluated by Mable et al. as putative Pickering emulsifiers.<sup>72</sup> As expected, the  $\text{PGMA}_{63}\text{-PHPMA}_{350}$  precursor vesicles did not survive the high shear conditions required to generate Pickering emulsions. In contrast,  $\text{PGMA}_{63}\text{-PHPMA}_{350}\text{-PBzMA}_z$  vesicles led to the formation of genuine Pickering emulsions, as confirmed by laser diffraction and TEM studies.<sup>72</sup> Moreover, the strongly hydrophobic nature of the third PBzMA block proved to be sufficient to prevent vesicle dissociation. Turbidimetric analysis of the lower aqueous phase after emulsion creaming was again used to assess the Pickering emulsifier performance of these framboidal vesicles. Systematic variation of the DP ( $z$ ) of the PBzMA block enabled their surface roughness to be tuned, which enabled the adsorption efficiency to be determined as a function of surface roughness (see Figure 9c) Increasing the PBzMA DP ( $z$ ) from 25 to 125 at a constant copolymer concentration led to an increase in

adsorption efficiency from 36% to 94%. Furthermore, framboidal vesicles with optimal surface roughness exhibited significantly higher adsorption efficiency than that observed for non-framboidal PGMA<sub>63</sub>-PHPMA<sub>350</sub>-PEGDMA<sub>20</sub> cross-linked vesicles (67%).<sup>187</sup>

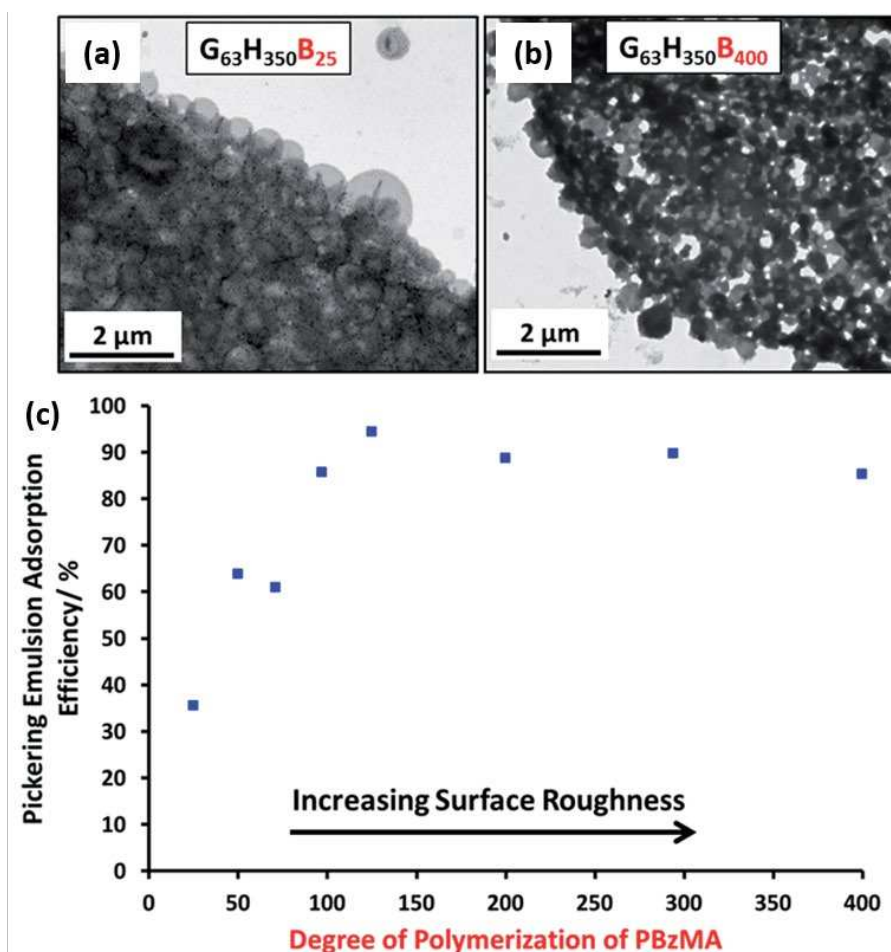


**Figure 9.** TEM images obtained for Pickering emulsions of *n*-dodecane stabilized using aqueous dispersions of (a) PGMA<sub>63</sub>-PHPMA<sub>350</sub>-PBzMA<sub>25</sub> and (b) PGMA<sub>63</sub>-PHPMA<sub>350</sub>-PBzMA<sub>400</sub> vesicles. (c) Variation of Pickering emulsion adsorption efficiency ( $A_{eff}$ ) against PBzMA DP for a series of PGMA<sub>63</sub>-PHPMA<sub>350</sub>-PBzMA vesicles of increasing surface roughness. Reproduced from ref. 72 (Copyright 2015 Royal Society of Chemistry).

Another example of framboidal vesicles was reported by Xiu and co-workers.<sup>181</sup> In this case, PGMA-PHPMA precursor vesicles were chain-extended using GlyMA *via* seeded RAFT aqueous emulsion polymerization, resulting in the formation of epoxy-functional framboidal vesicles. Such framboidal vesicles were shown to be an efficient Pickering emulsifier for *n*-hexane-in-water emulsions, with higher PGlyMA DPs and copolymer concentrations leading to the formation of finer oil droplets.

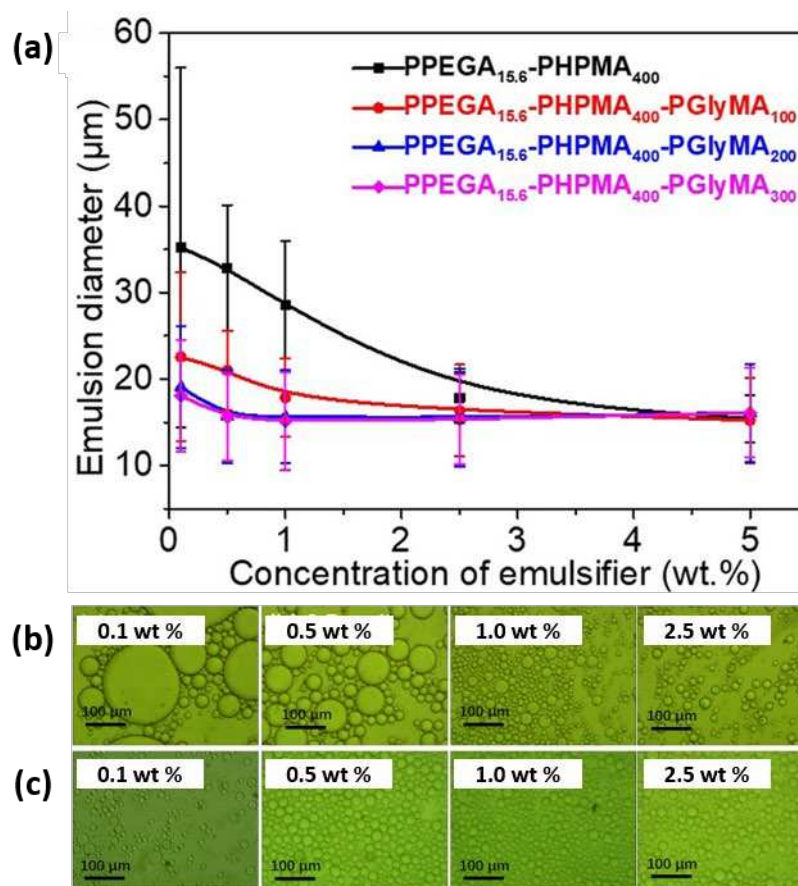


**Figure 10.** (a) Effect of varying the copolymer concentration on the mean droplet diameter of Pickering emulsions prepared using PPEGA<sub>15.6</sub>-PHPMA<sub>400</sub>-PGlyMA<sub>n</sub> multicompartement block copolymer nanoparticles (MBCPs). Optical microscopy images recorded for *n*-hexane-in-water emulsions stabilized using (b) PPEGA<sub>15.6</sub>-PHPMA<sub>400</sub> precursor nanoparticles and (c) epoxy-functionalized PPEGA<sub>15.6</sub>-PHPMA<sub>400</sub>-PGlyMA<sub>300</sub> nanoparticles at the stated copolymer concentrations. Reproduced from ref. 210 (Copyright 2019 American Chemical Society).

The same research group also evaluated so-called multicompartement block copolymer nanoparticles (MBCPs) as Pickering emulsifiers.<sup>210</sup> Such nanoparticles were prepared *via* photoinitiated PISA in a two-step synthesis. First, a poly(poly(ethylene glycol) methyl ether acrylate) (PPEGA) precursor was chain-extended via RAFT aqueous dispersion polymerization of HPMA to yield well-defined spheres. Such spheres were then chain-extended using GlyMA to produce MBCP nanoparticles. The Pickering performance of the precursor PPEGA<sub>15.6</sub>-PHPMA<sub>400</sub> spheres was compared to that of the final PPEGA<sub>15.6</sub>-PHPMA<sub>400</sub>-PGlyMA<sub>n</sub> particles, which had a distinctly framboidal morphology. There was an upturn in the mean droplet diameter at lower copolymer concentrations, indicating the formation of genuine Pickering emulsions (see Figure 10). As previously discussed, PHPMA-

core diblock copolymer nanoparticles typically dissociate to form individual copolymer chains during high shear homogenization.<sup>72, 187-188, 194</sup> In contrast, laser diffraction data suggested that the PPEGA<sub>15.6</sub>-PHPMA<sub>400</sub> precursor nanoparticles survive emulsification intact.<sup>211</sup> Increasing the DP of the PGlyMA block up to 300 led to greater surface roughness, lower limiting copolymer concentrations and the formation of finer emulsion droplets for a given copolymer concentration.

A summary of the majority of the block copolymer nano-objects discussed in this section and their Pickering emulsifier performance is shown in Table 1.

**Table 1. Summary of Pickering emulsions prepared using block copolymer nanoparticles of differing morphologies.**

block copolymer composition	copolymer morphology	Linear or cross-linked?	emulsion type	Genuine Pickering emulsion?	Ref.
PGMA <sub>45</sub> -PHPMA <sub>200</sub>	vesicular	linear	o/w	no	187
PGMA <sub>58</sub> -PHPMA <sub>350</sub> -PEGDMA <sub>20</sub>	vesicular	cross-linked	o/w	yes	187
PGMA <sub>63</sub> -PHPMA <sub>350</sub> -PBzMA <sub>25</sub>	vesicular	linear	o/w	yes	72
PPEGA <sub>15.6</sub> -PHPMA <sub>400</sub> -PGlyMA <sub>300</sub>	multicompartmental	linear	o/w	yes	210
PGMA <sub>100</sub> -PHPMA <sub>200</sub> -PEGDMA <sub>20</sub>	spherical	cross-linked	o/w	yes	188
PGMA <sub>45</sub> -PHPMA <sub>140</sub>	worm-like	linear	o/w	no	188
PGMA <sub>45</sub> -PHPMA <sub>100</sub> -PEGDMA <sub>10</sub>	worm-like	cross-linked	o/w	yes	188
PGMA <sub>51</sub> -PBzMA <sub>50</sub>	spherical	linear	o/w	yes	188
PGMA <sub>37</sub> -PHPMA <sub>60</sub> -PBzMA <sub>30</sub>	worm-like	linear	o/w	yes	188
PNMP <sub>53</sub> -PFMA <sub>5</sub>	spherical	linear	o/w	Depends on shear-rate	206
PNMP <sub>53</sub> -PFMA <sub>10</sub>	worm-like	linear	o/w	yes	206
PGMA <sub>48</sub> -P(HPMA <sub>90</sub> -stat-GlyMA <sub>15</sub> )	short worms	cross-linked	o/w	yes	194
PGMA <sub>48</sub> -P(HPMA <sub>90</sub> -stat-GlyMA <sub>15</sub> )	long worms	cross-linked	o/w	yes	194
PLMA <sub>16</sub> -PBzMA <sub>37</sub>	worm-like	linear	w/o	yes	189
PLMA <sub>16</sub> -PBzMA <sub>37</sub>	spherical	linear	w/o	yes	189

## DESIGN OF PICKERING EMULSIFIERS WITH TUNABLE SURFACE

### WETTABILITY

Using either hydrophilic or hydrophobic stabilizer blocks enables PISA to be conducted in either polar or non-polar solvents. As already noted, the chemical nature of the stabilizer block directly influences the surface wettability of such block copolymer nanoparticles and therefore dictates the type of Pickering emulsion that is formed. For example, PGMA-stabilized spheres, worms or vesicles invariably stabilize oil-in-water emulsions.<sup>72-73, 117, 187, 191</sup> Clearly, the hydrophilic PGMA chains produce a three-phase particle contact angle of less than 90°. In contrast, the core-forming block has little or no influence over surface wettability of such particles, with o/w Pickering emulsions being obtained when using either weakly hydrophobic (cross-linked) PHPMA cores<sup>187-188</sup> or strongly hydrophobic cores such as PBzMA.<sup>117</sup> On the other hand, using a highly hydrophobic stabilizer block such as PLMA or poly(stearyl methacrylate) (PSMA) almost invariably leads to the formation of w/o Pickering emulsions.<sup>73-74, 189, 212</sup> Such nanoparticles are preferentially wetted by the oil to produce a three-phase contact angle of more than 90°.

Thompson et al. used hydrophobic PLMA<sub>16</sub>-PBzMA<sub>37</sub> worms in conjunction with hydrophilic PGMA<sub>37</sub>-PHPMA<sub>60</sub>-PBzMA<sub>30</sub> worms to prepare Pickering double emulsions.<sup>73</sup> Figure 11 shows how either water-in-oil-in-water (w/o/w) or oil-in-water-in-oil (o/w/o) Pickering double emulsions could be obtained depending on the emulsification protocol. The former emulsions were obtained by first preparing a precursor w/o emulsion stabilized using PLMA<sub>16</sub>-PBzMA<sub>37</sub> worms. A relatively high stirring rate of 24,000 rpm was chosen to generate the smallest possible mean droplet diameter. Subsequently, this w/o emulsion was then homogenized with an equal volume of an aqueous dispersion of PGMA<sub>37</sub>-PHPMA<sub>60</sub>-PBzMA<sub>30</sub> worms. A lower stirring rate of 7,000 rpm was used in this step to produce larger aqueous droplets and hence favor formation of the desired w/o/w Pickering double emulsion.

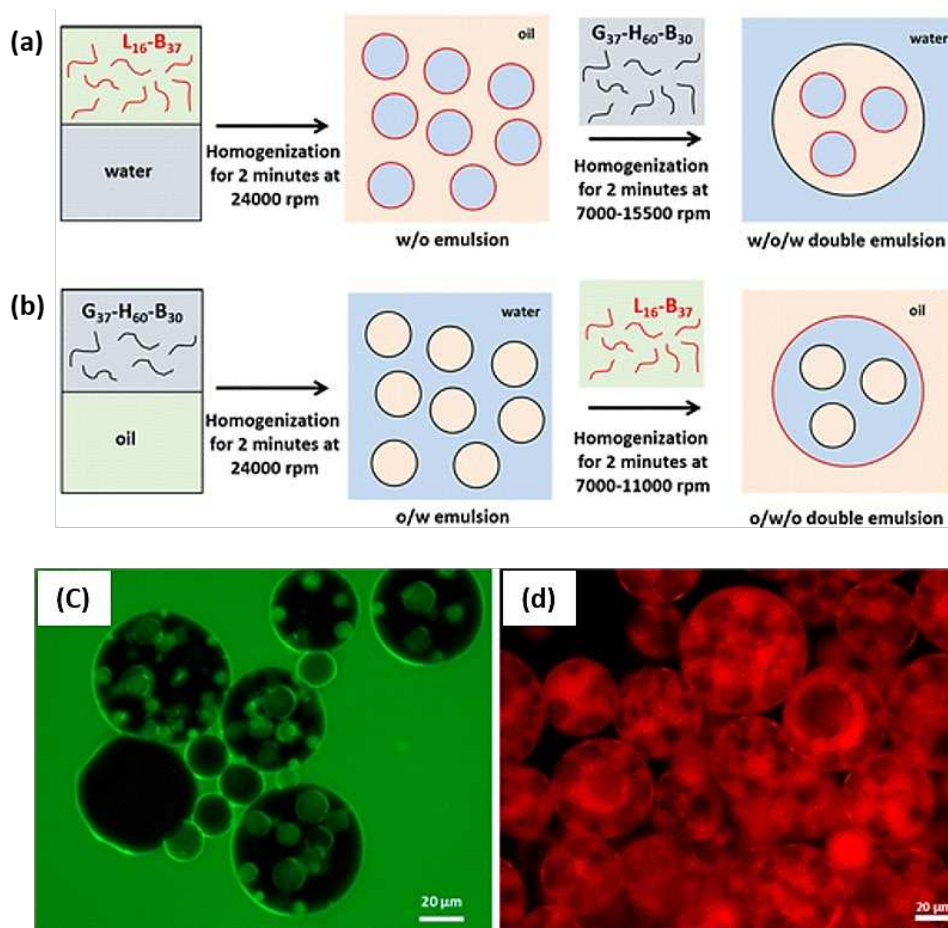


**Figure 11.** Schematic representation of the preparation of (a) w/o/w double emulsions and (b) o/w/o double emulsions by the judicious combination of the two types of highly anisotropic block copolymer worms as Pickering emulsifiers. Fluorescence microscopy images confirm the successful formation of w/o/w Pickering double emulsions where (c) the aqueous phase is labeled with fluorescein and (d) the *n*-dodecane phase is labeled with Nile Red. Reproduced from ref. 73 (Copyright 2015 American Chemical Society).

Similarly, o/w/o Pickering double emulsions could be prepared by first homogenizing a precursor o/w emulsion stabilized using PGMA<sub>37</sub>-PHPMA<sub>60</sub>-PBzMA<sub>30</sub> worms, followed by its homogenization with an equal volume of *n*-dodecane containing PLMA<sub>16</sub>-PBzMA<sub>37</sub> worms.

More recently, Rymaruk and co-workers reported that a range of poly(3-[tris(trimethylsiloxy)silyl]propyl methacrylate)-poly(benzyl methacrylate) (PSiMA-PBzMA) spheres could be prepared directly in a low-viscosity silicone oil (DM5).<sup>213</sup> Such sterically-stabilized nanoparticles were evaluated as Pickering emulsifiers for ten bio-sourced oils. For three of these oils, using a copolymer concentration of 2.0% w/w and a DM5 volume fraction

of 0.50 led to the formation of oil-in-oil Pickering emulsions, with DM5 forming the continuous phase in each case (Figure 12a). Such emulsions remained stable for at least two months when stored at 20 °C. To improve the Pickering emulsifier performance of such P*SiMA*-stabilized spheres, lauryl methacrylate (LMA) was statistically copolymerized with BzMA when preparing the core-forming block. The resulting optimized P*SiMA*<sub>19</sub>-P(BzMA<sub>190</sub>-*stat*-LMA<sub>10</sub>) nanoparticles enabled the formation of stable oil-in-oil emulsions when using nine of the ten bio-sourced oils, as shown in Figure 12b.

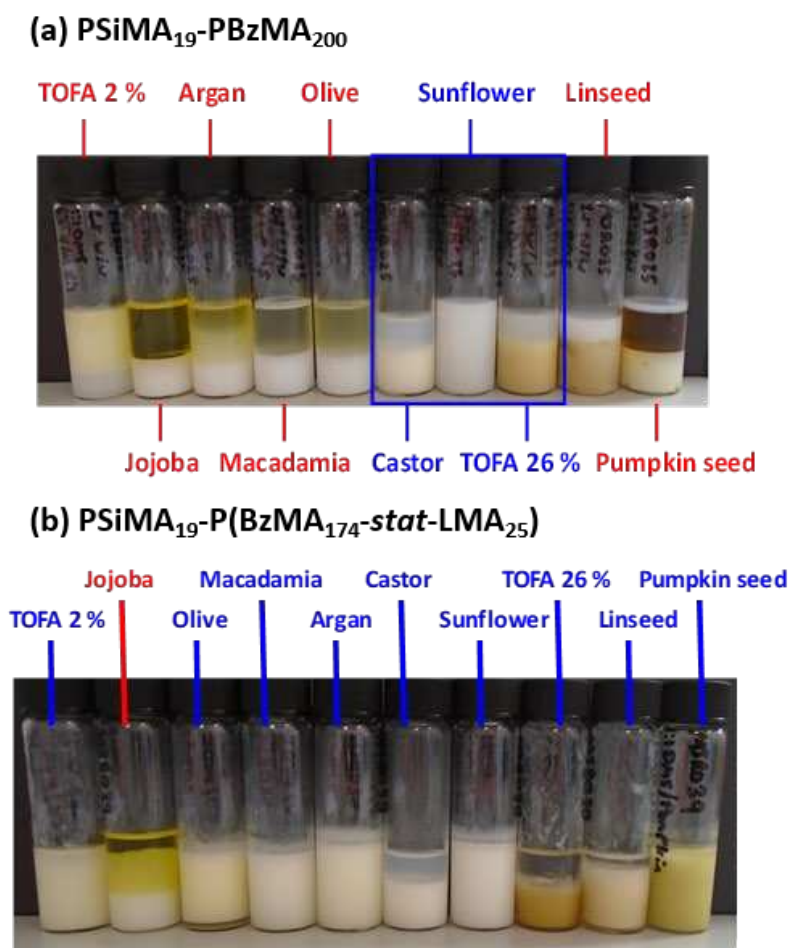


**Figure 12.** (a) Digital photograph recorded after standing for two months at 20 °C showing various bio-sourced oil-in-oil Pickering emulsions prepared using a 2.0% w/w dispersion of P*SiMA*<sub>19</sub>-P*BzMA*<sub>200</sub> spheres in a silicone oil (DM5). Each bio-sourced oil is indicated above or below the relevant vial: emulsions that remained stable after two months are denoted in blue, whereas those that undergo (partial) phase separation on this time scale are shown in red. (b) Digital photograph of various oil-in-DM5 Pickering emulsions prepared using a 2.0% w/w dispersion of P*SiMA*<sub>19</sub>-P(BzMA<sub>174</sub>-*stat*-LMA<sub>25</sub>) spheres in DM5 recorded after storage for two months at 20 °C. In each case, the DM5 volume fraction was 0.50 and the P*SiMA*<sub>19</sub>-P(BzMA<sub>175</sub>-*stat*-LMA<sub>25</sub>) concentration was 2.0% w/w. Emulsions that remained stable after two months are indicated in blue, whereas the single jojoba oil-based emulsion that underwent phase separation over this time period is shown in red. Reproduced from ref. 213 (Copyright 2020 Elsevier).

This was attributed to enhanced wettability of the nanoparticles by the bio-sourced oil, thus leading to stronger interfacial adsorption. This study clearly demonstrates that the chemical nature of the *core-forming* block can influence the surface wettability of block copolymer nanoparticles, in addition to that of the *stabilizer* block.

An and co-workers prepared oil-in-oil HIPEs from semi-fluorinated block copolymer nanoparticles.<sup>214</sup> Spherical diblock copolymer nanoparticles were initially prepared in DMF *via* RAFT dispersion polymerization of heptadecafluorodecyl methacrylate (HDFDMA) using a PMMA<sub>43</sub> precursor. Such PMMA<sub>43</sub>-PHDFDMA<sub>50</sub> nanoparticles were transferred into DMSO and subsequently subjected to high shear homogenization with cyclohexane (volume fraction = 0.80). This led to the formation of a highly viscous cyclohexane-in-DMSO HIPE. This is an example of non-aqueous HIPE which have rarely been reported.<sup>215-216</sup> In the same study, PSMA<sub>15</sub>-PHDFDMA<sub>50</sub> short rods were prepared *via* RAFT dispersion polymerization in *n*-dodecane. A 5% w/w dispersion of such nanoparticles could be used to prepare relatively stable DMF-in-*n*-dodecane Pickering emulsion by homogenization with an equivalent volume of DMF. This is a rather rare example of such an emulsion, not least because these two solvents are usually considered to be miscible.<sup>217</sup>

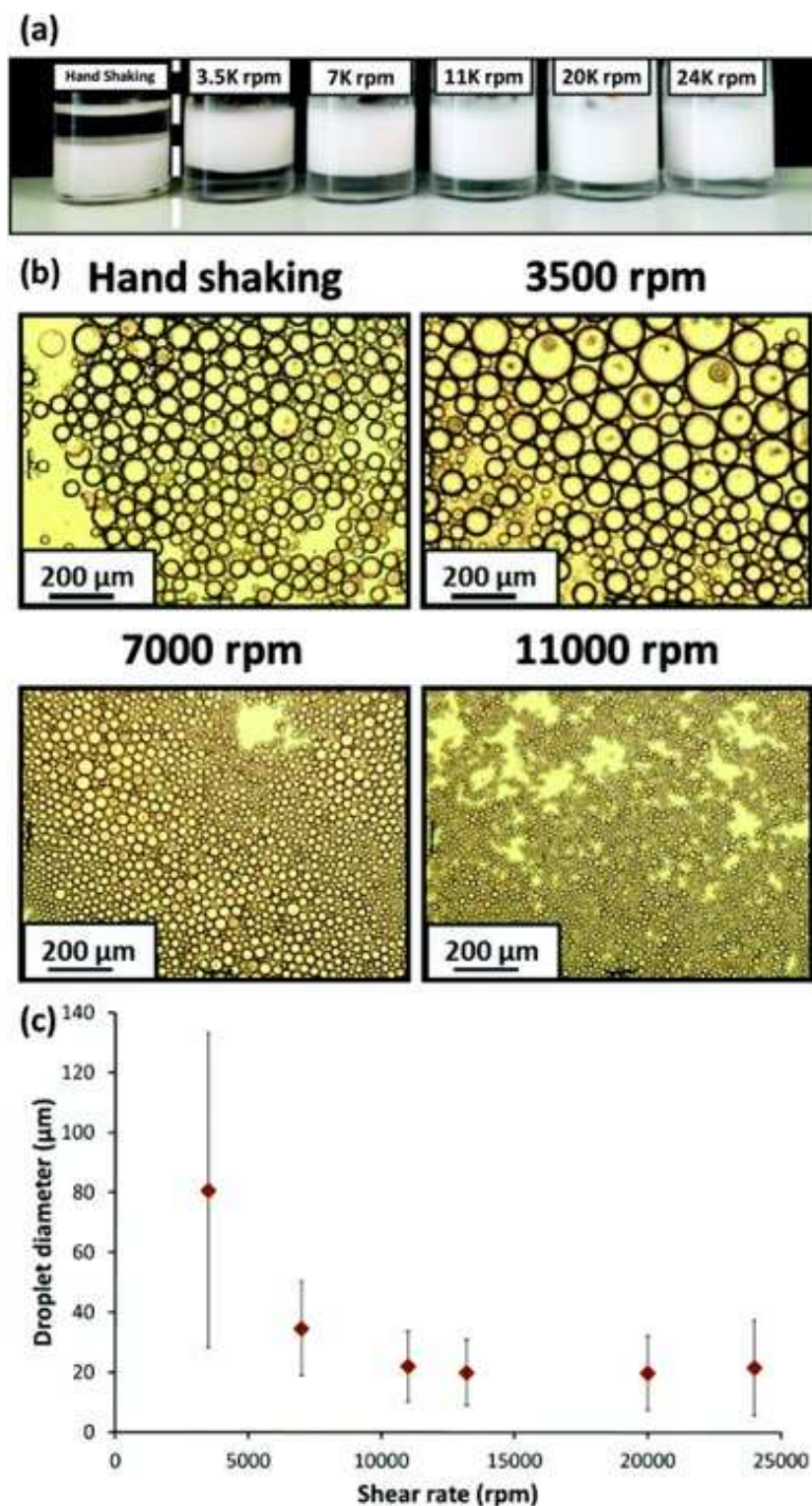


**Figure 13.** (a) Digital photographs obtained for the Pickering emulsions prepared using 1.0% w/w PSMA<sub>14</sub>-PNMEP<sub>49</sub> spherical nanoparticles at various shear rates. Oil-in-water emulsions are formed in all cases, except when hand-shaking is used; this latter approach instead results in the formation of a water-in-oil emulsion. (b) Optical microscopy images recorded for the droplets prepared *via* hand-shaking, or *via* homogenization at 3,500 rpm, 7,000 rpm or 11,000 rpm (scale bar = 200 μm). (c) Shear rate dependence for the mean droplet diameter (as determined by laser diffraction) of Pickering emulsions prepared using PSMA<sub>14</sub>-PNMEP<sub>49</sub> spheres as the sole emulsifier. The error bars represent the standard deviation of each volume-average droplet diameter, rather than the experimental error. Reproduced from ref. 212 (Copyright 2016 Royal Society of Chemistry).

In general, block copolymer nanoparticles comprising a hydrophilic stabilizer block are expected to produce o/w emulsions, while those prepared with a hydrophobic stabilizer block should afford w/o emulsions. However, block copolymer nanoparticles prepared by RAFT dispersion polymerization in non-polar oils comprising a relatively hydrophilic core-forming block do not appear to follow this general rule. For example, Cunningham and co-workers reported that poly(stearyl methacrylate)–poly(*N*-2-(methacryloyloxy)ethyl pyrrolidone) (PSMA<sub>14</sub>–PNMEP<sub>49</sub>) spheres prepared in *n*-dodecane could form either w/o or o/w Pickering emulsions depending on the emulsification conditions.<sup>212</sup> Thus, o/w emulsions were obtained when conducting high shear homogenization with an equal volume fraction of water at 3,500–24,000 rpm, whereas emulsification by hand-shaking led to w/o emulsions. This unexpected result was attributed to *in situ* inversion of the nanoparticles during homogenization to form hydrophilic PNMEP<sub>49</sub>-PSMA<sub>14</sub> block copolymer spheres. As expected, increasing the shear rate led to a reduction in the main oil droplet diameter (see Figure 13c). Increasing the oil volume fraction from 50% v/v up to 75% v/v prevented nanoparticle inversion and hence enabled the formation of w/o Pickering emulsions.

In a related study by György et al., the Pickering emulsifier behavior of PSMA<sub>12</sub>-PHPMA<sub>50</sub> spheres was explored.<sup>218</sup> In this case, the relatively polar PHPMA core-forming block is not actually water-soluble, hence different emulsifier behavior was anticipated. In this case, the emulsion type depended on the water volume fraction. At relatively low water volume fractions (0.125 – 0.375), w/o Pickering emulsions were obtained at 1.0% w/w copolymer concentration. However, using water volume fractions of 0.50 – 0.75 led to formation of a w/o/w Pickering double emulsion, as confirmed by fluorescence microscopy. Thus, this is a rare example of a double emulsion that can be prepared using a *single* copolymer composition.

## STABILIZATION OF GIANT PICKERING DROPLETS

In recent years, there have been a number of reports of particle-stabilized droplets of the order of 1-2 mm diameter.<sup>190, 195, 219-226</sup> Such ‘giant’ Pickering emulsions are typically prepared using capillaries and can act as model systems to provide useful insights into coalescence behavior<sup>221</sup> and particle adsorption kinetics.<sup>195</sup> The use of spherical latex particles to stabilize ‘giant’ Pickering emulsions has been studied in some detail.<sup>220</sup> Thompson et al. used conventional free radical polymerization to prepare PGMA-stabilized polystyrene latexes of either 135 nm or 905 nm diameter *via* aqueous emulsion or alcoholic dispersion polymerization, respectively.<sup>221</sup> Such latexes were then used to prepare millimeter-sized *n*-dodecane droplets. High speed video imaging was used to monitor the coalescence of these latex-coated droplets.<sup>219</sup> Longer coalescence times were observed for Pickering emulsions prepared using the 902 nm latex and either bilayer formation or a bridging monolayer occurred prior to coalescence.<sup>221</sup> Giant colloidosomes were produced by adding an oil-soluble cross-linker (PPG-TDI) to the oil phase (sunflower oil) prior to droplet formation.<sup>221</sup> Cross-linking for 20 min at 25 °C led to a reduction in the interfacial elasticity and prevented any droplet coalescence. In contrast, giant oil droplets coated with charge-stabilized poly(*tert*-butylamino)ethyl methacrylate (PTBAEMA) latex particles coalesced on close contact in the absence of any PPG-TDI cross-linker.<sup>224</sup>

Block copolymer nanoparticles prepared *via* PISA have also been used as emulsifiers for millimeter-sized droplets.<sup>190, 195</sup> As previously discussed, linear PGMA-PHPMA block copolymer worms are unstable with respect to nanoparticle dissociation when subjected to high shear homogenization. However, a highly hydrophobic block (e.g. PBzMA) can be added to the nanoparticle cores to confer stability. Thus, Mable et al. prepared linear PGMA-PHPMA-PBzMA triblock copolymer worms *via* RAFT-mediated PISA.<sup>190</sup> Such worms were evaluated as Pickering emulsifiers for the stabilization of o/w emulsions prepared under low

shear conditions (i.e. hand-shaking). Optical microscopy and laser diffraction studies confirmed that the worms survived such emulsification conditions and adsorbed intact at the oil/water interface. Much larger millimeter-sized oil droplets were produced using hand-shaking compared to those using high shear homogenization. In contrast to the PGMA-*PHPMA*-*PBzMA* worms, droplet diameters for emulsions prepared using PGMA-*PHPMA* worms remained relatively constant with increasing copolymer concentration. This indicates that such worms dissociate even during low shear emulsification, generating individual amphiphilic diblock copolymer chains adsorbed at the oil/water interface, rather than nanoparticles.

Subsequently, Cunningham et al. used either 22 nm diameter *PGMA*<sub>39</sub>-*PBzMA*<sub>60</sub> spheres or *PGMA*<sub>37</sub>-*PHPMA*<sub>60</sub>-*PBzMA*<sub>30</sub> worms (mean worm width = 26 nm) in turn to stabilize millimeter-sized *n*-dodecane droplets.<sup>195</sup> Dynamic interfacial tension measurements were conducted to assess the kinetics of adsorption for these two morphologies. In both cases, a rapid initial reduction in interfacial tension occurred within 20 s, with a more gradual but still significant reduction being observed thereafter. This provided direct evidence for nanoparticle adsorption at the oil/water interface and suggested the possibility of post-adsorption nanoparticle reorganization. The worms lowered the interfacial tension significantly more than the spheres, indicating that the former had a stronger affinity for the *n*-dodecane/water interface. Both spheres and worms stabilized ‘giant’ Pickering droplets but the former proved to be more effective at stabilizing the interface in the absence of any interfacial ageing. This was attributed to the very high capillary pressure generated by such small nanoparticles. In contrast, the significantly larger worms required interfacial ageing for at least 90 s before droplet stability was achieved owing to their slower diffusion to the interface and rearrangement after initial adsorption. Systematic variation of the copolymer concentration revealed that the worms were able to stabilize ‘giant’ Pickering emulsions at

lower concentrations than the equivalent 22 nm spheres. Finally, the effect of mean sphere diameter on droplet coalescence time was examined for 22, 41, 60 and 91 nm PGMA<sub>39</sub>-PBzMA<sub>x</sub> spheres (see Figure 14). Stable droplets were obtained using either 22 nm or 41 nm spheres, but coalescence was always observed when using 60 nm and 91 nm spheres, even after relatively long ageing times. Presumably, this reduction in droplet stability is related to the lower capillary pressure for such larger particles, since all other parameters remained constant.

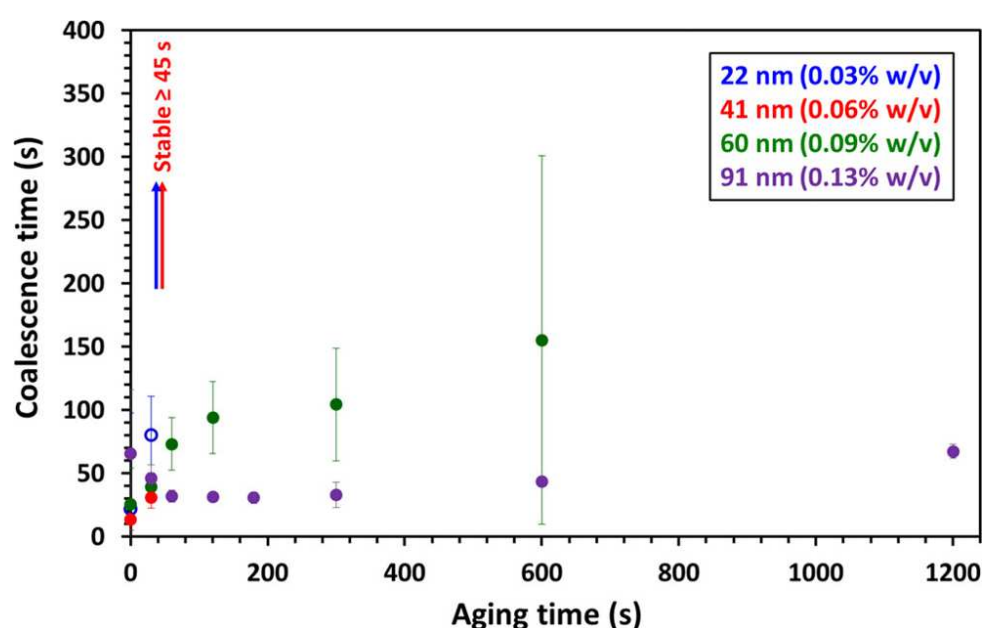


**Figure 14.** Coalescence time vs. ageing time plot for two *n*-dodecane droplets grown in the presence of dilute aqueous dispersions of PGMA<sub>39</sub>-PBzMA<sub>x</sub> spheres of varying mean diameter. Open markers indicate conditions for which, in some cases, droplets were stable toward coalescence for at least 30 min. Reproduced from ref. 195 (Copyright 2017 American Chemical Society).

## PICKERING NANOEMULSIONS

Nanoemulsions comprise stable oil or water droplets for which the mean droplet diameter is below 200 nm.<sup>227-228</sup> There are various reports of copolymer- or surfactant-stabilised nanoemulsions in the literature.<sup>229</sup> In contrast, there have been remarkably few examples of Pickering nanoemulsions, in which the droplets are solely stabilized by solid particles.<sup>192-193, 230-233</sup> No doubt one reason for the paucity of studies is the rule-of-thumb requirement that the Pickering emulsifier should be at least 5-10 times smaller than the mean

droplet diameter. However, the recent development of polymerization-induced self-assembly (PISA) has enabled the highly convenient synthesis of sterically-stabilized diblock copolymer spheres of 20-25 nm diameter directly in the form of concentrated aqueous dispersions.<sup>117, 234</sup> In principle, such nanoparticles should constitute model Pickering emulsifiers for oil-in-water nanoemulsions.

For example, Thompson and co-workers chain-extended a water-soluble PGMA<sub>48</sub> precursor *via* RAFT aqueous emulsion polymerization of 2,2,2-trifluoroethyl methacrylate (TFEMA) to form PGMA<sub>48</sub>-PTFEMA<sub>50</sub> spheres of approximately 25 nm diameter,<sup>192</sup> as previously reported by Akpinar and co-workers.<sup>234</sup> As discussed above, the hydrophobic character of the core-forming block is of critical importance when preparing Pickering emulsions using block copolymer nanoparticles. Selecting a weakly hydrophobic block such as PHPMA usually means that the nanoparticles do not survive the high shear homogenization conditions required for droplet formation. On the other hand, nanoparticles with highly hydrophobic core-forming blocks such as PTFEMA typically remain intact and therefore can act as genuine Pickering emulsifiers. Indeed, this criterion is particularly important for the formation of Pickering nanoemulsions because even more energy-intensive conditions are required.

Initially, a Pickering macroemulsion of approximately 40  $\mu\text{m}$  diameter was prepared *via* high shear homogenization of a 7.0% w/w aqueous dispersion of PGMA<sub>48</sub>-PTFEMA<sub>50</sub> spheres with *n*-dodecane at 15,500 rpm. Employing a relatively high copolymer concentration during this stage was deliberate because a large excess of non-adsorbed nanoparticles was required to stabilize the nanoemulsion generated in the second stage. Such precursor emulsions were then subjected to high pressure microfluidization to generate much finer droplets (see Figure 15). The final size of the oil droplets depended on both the applied pressure and also the number of passes through the microfluidizer. At least eight passes were



Subtracting the thickness of the adsorbed monolayer of 25 nm PGMA<sub>48</sub>-PTFEMA<sub>50</sub> spheres indicates a mean oil droplet diameter of less than 200 nm, which lies within the range required for a genuine nanoemulsion. Moreover, such nanoparticles enabled the formation of high internal phase nanoemulsions at oil volume fractions of up to 0.80. However, TEM analysis of dried nanoemulsion droplets prepared at 30,000 psi revealed no evidence of the original nanoparticles. At this higher applied pressure, nanoparticle dissociation occurred and the molecularly dissolved PGMA<sub>48</sub>-PTFEMA<sub>50</sub> chains copolymer acted as an amphiphilic polymeric surfactant. This problem could be circumvented by incorporating EGDMA as a third block: the resulting covalently-stabilized PGMA<sub>48</sub>-PTFEMA<sub>45</sub>-PEGDMA<sub>5</sub> remained intact even at an applied pressure of 30,000 psi, thus ensuring the formation of genuine Pickering emulsions under such conditions.

In a follow-up study, Thompson et al. examined the effect of varying the oil type on the long-term stability of Pickering nanoemulsions prepared using the same PGMA<sub>48</sub>-PTFEMA<sub>50</sub> nanoparticles.<sup>193</sup> Thus, a series of nanoemulsions prepared using four *n*-alkanes were prepared using an LV1 microfluidizer and their relative long-term stabilities were assessed using analytical centrifugation.<sup>31</sup> More specifically, a LUMiSizer instrument was employed to size the ageing droplets over a six-week period, see Figure 16. Significant broadening of the droplet size distribution was observed in each case, although the change in mean droplet diameter was minimal. For the more stable nanoemulsions prepared using *n*-tetradecane or *n*-dodecane, over 90% of the droplets remained below 1  $\mu\text{m}$  after six weeks. Conversely, nanoemulsions prepared using *n*-octane proved to be relatively unstable, which correlates with the higher water solubility of this oil.

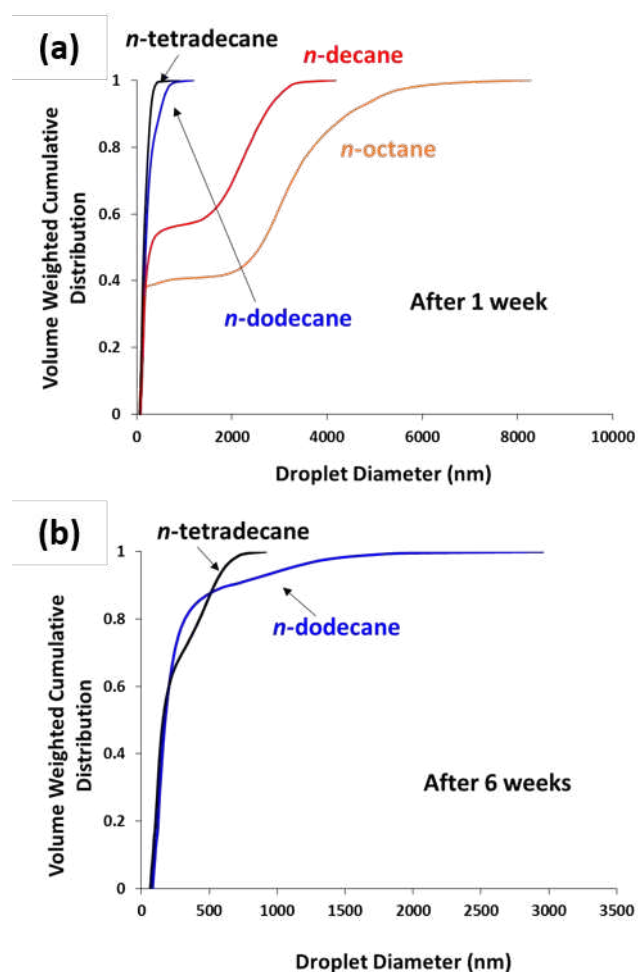


**Figure 16.** Volume-weighted cumulative distributions determined by analytical centrifugation (LUMiSizer instrument) for a series of four *n*-alkane-in-water Pickering nanoemulsions: (a) after ageing for one week at 20 °C and (b) after ageing for six weeks. Significant evaporation of the more volatile *n*-octane and *n*-decane oils occurred within one week so no further analysis was possible in these two cases. Reproduced from ref. 193 (Copyright 2018 American Chemical Society).

We recently explored the effect of introducing charge at the end of the steric stabilizer block on the formation and long-term stability of Pickering nanoemulsions prepared using PGMA<sub>48</sub>-PTFEMA<sub>50</sub> nanoparticles.<sup>232</sup> RAFT-mediated PISA enables the design of block copolymer nanoparticles with minimal surface charge by simply selecting an appropriate RAFT agent when preparing the steric stabilizer precursor. Hence PGMA chains bearing either carboxylic acid, morpholine or neutral end-groups were chain-extended by RAFT aqueous emulsion polymerization of TFEMA. Thus ionization of the carboxylic acid group at neutral pH introduced terminal anionic charge, whereas protonation of the tertiary amine group at low pH conferred cationic charge. Analysis of the aqueous phase after

microfluidization phase by gel permeation chromatography using a UV detector enabled convenient quantification of the nanoparticle adsorption efficiency. Up to 90% of the neutral nanoparticles were adsorbed at the surface of the oil droplets. In contrast, introducing either anionic or cationic charge at the stabilizer chain-ends significantly reduced the nanoparticle adsorption efficiency. Moreover, SAXS studies indicated that the packing efficiency of neutral nanoparticles at the oil/water interface was significantly higher than that of nanoparticles bearing charged end-groups. Analytical centrifugation was used to evaluate the long-term stability of such Pickering nanoemulsions. Pickering nanoemulsions prepared using nanoparticles bearing charged end-groups proved to be significantly less stable than those bearing neutral end-groups. Figure 17 shows droplet size distributions recorded for both freshly prepared and one-week-old Pickering nanoemulsions. If the adsorbed nanoparticles were in their neutral state, then the droplet size distribution became bimodal. On the other hand, if the same nanoparticles possessed charged end-groups then larger droplets were produced on ageing but the size distribution remained unimodal.

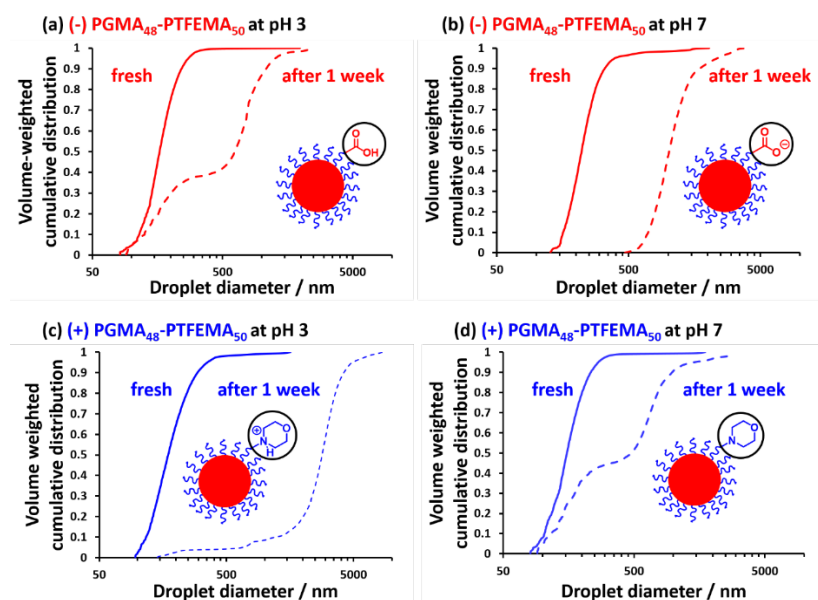


**Figure 17.** Volume-weighted cumulative size distributions determined by analytical centrifugation (LUMiSizer instrument) for fresh (solid line) and aged (for one week at 20 °C, dashed line) *n*-dodecane-in-water Pickering nanoemulsions prepared using 7.0% w/w PGMA<sub>48</sub>-PTFEMA<sub>50</sub> nanoparticles prepared using: (a) a carboxylic acid-based RAFT agent aged at pH 3; (b) the same carboxylic acid-based RAFT agent aged at pH 7; (c) a morpholine-based RAFT agent aged at pH 3; (d) the same morpholine-based RAFT agent aged at pH 7. Microfluidizer conditions: 20,000 psi; ten passes. Reproduced from ref. 232 (Copyright 2020 American Chemical Society).

## TRANSPARENT PICKERING EMULSIONS

It is well-known that emulsions usually possess high turbidity owing to strong light scattering by the droplet phase. However, according to Snell's law an emulsion should be transparent if the continuous phase and the droplet phase possess identical refractive indices.<sup>235</sup> For surfactant-stabilized emulsions, the emulsifier is far too small to cause any additional light scattering so examples of highly transparent conventional emulsions are not uncommon.<sup>235-237</sup> On the other hand, the design of transparent Pickering emulsions is much more challenging owing to additional light scattering arising from the adsorbed particles.<sup>71, 191</sup> In this case, the droplet phase, continuous phase and the Pickering emulsifier must possess precisely the same refractive index to eliminate light scattering and achieve high transparency. In principle, the refractive index of block copolymer nanoparticles prepared *via* PISA can be tuned by simply varying the copolymer composition. Thus, such nanoparticles are strong candidates for the design of transparent emulsions. However, the refractive index of water (1.33) lies well below that of most oils. Thus, either water-soluble or water-miscible species must be added to the aqueous phase to raise its refractive index to that of the oil phase.

In an alternative approach, Thompson and co-workers reported the preparation of an almost isorefractive *non-aqueous* Pickering emulsion using diblock copolymer worms.<sup>71</sup> This formulation comprised ethylene glycol-in-*n*-tetradecane emulsions stabilized by PLMA<sub>16</sub>-PBzMA<sub>37</sub> worms. These two immiscible liquids were selected owing to their almost identical refractive index (~1.43). However, the core-forming PBzMA block has a relatively high refractive index of 1.57 so such emulsions are only translucent (transmittance = 70-80%, depending on the precise wavelength of visible light) owing to weak light scattering by the adsorbed worms.

Subsequently, Rymaruk et al. demonstrated that highly transparent Pickering double emulsions could be prepared by selecting a model oil, designing suitable diblock copolymer

nanoparticles and employing an appropriate concentration of a water-soluble additive.<sup>191</sup> Semi-fluorinated PTFEMA was selected as the core-forming block owing to its relatively low refractive index of 1.42, which almost perfectly matches that of *n*-dodecane. Thus, judicious addition of either 50.5% sucrose or 67% glycerol to an aqueous dispersion of PGMA<sub>56</sub>-PTFEMA<sub>500</sub> nanoparticles, followed by homogenization with *n*-dodecane, produced a highly transparent *n*-dodecane-in-water Pickering emulsion, as shown in Figure 18. Moreover, complementary water-in-*n*-dodecane Pickering emulsions of similarly high transmittance could be prepared by using hydrophobic PLMA<sub>39</sub>-PTFEMA<sub>800</sub> nanoparticles prepared via PISA in *n*-dodecane. Finally, combining these hydrophilic and hydrophobic nanoparticles enabled the preparation of an o/w/o Pickering double emulsion that exhibited a mean transmittance of almost 90% across the visible spectrum. This study highlights the versatility and potential offered by PISA for the rational design of bespoke Pickering emulsifiers of tunable size and surface chemistry.

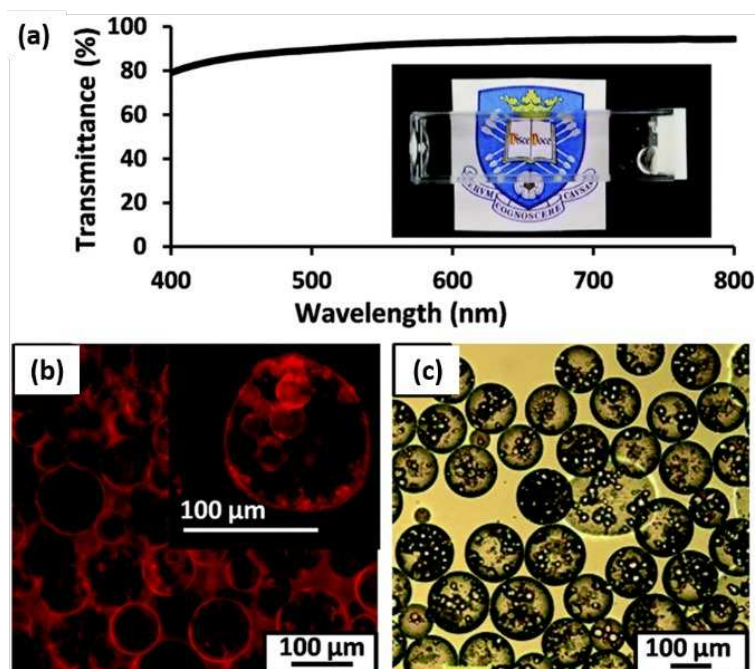


**Figure 18.** (a) Transmittance % vs. wavelength plot recorded for an *n*-dodecane-in-50.5% aqueous sucrose-in-*n*-dodecane Pickering double emulsion (inset: digital photograph illustrates the highly transparent nature of this refractive index-matched emulsion). (b) Fluorescence micrograph recorded for the same Pickering double emulsion prepared with Nile Red dye dissolved in the oil phase. (c) Optical micrograph obtained for the same emulsion prepared in the absence of any sucrose, i.e. with pure water, in order to provide contrast. Reproduced from ref. 191 (Copyright 2016 Royal Society of Chemistry).

## CONCLUSIONS AND PROSPECT

PISA enables the facile synthesis of a wide range of block copolymer nano-objects as concentrated dispersions in either water or various oils. The particle size, copolymer morphology and surface chemistry can be predicted by selecting appropriate steric stabilizer and structure-directing blocks and targeting the desired DPs. Many of these nano-objects can be used as model polymer-based Pickering emulsifiers that can be used to examine the effect of varying the particle size, morphology, surface roughness and surface charge. In principle, this enables the effect of varying such parameters on the interfacial surface tension, adsorption dynamics, interparticle forces and interfacial mechanics to be examined, although such model experimental studies are yet to be performed. In some cases, such Pickering emulsifiers may be prone to dissociate into individual amphiphilic copolymer chains during high shear homogenization. However, this technical problem can be addressed by either covalent stabilization or addition of a more solvophobic block such as PBzMA.<sup>72, 187-188, 194 117</sup> Recently, we have reported protocols for preparing sphere, worms and vesicles via RAFT aqueous emulsion polymerization of vinyl monomers that exhibit moderate aqueous solubility (15-20 g dm<sup>-3</sup>).<sup>238-240</sup> Such nano-objects are expected to act as new Pickering emulsifiers that are stable towards high shear emulsification without recourse to covalent stabilization. RAFT aqueous emulsion polymerization has also enabled the synthesis of relatively small block copolymer nanoparticles possessing highly hydrophobic cores. Such nanoparticles can be used to prepare model *n*-alkane-in-water Pickering nanoemulsions.<sup>192</sup> This has enabled systematic studies of the effect of varying (i) the *n*-alkane type<sup>193</sup> and (ii) the introduction of terminal ionic charge<sup>232</sup> on the rate of demulsification via Ostwald ripening. For example, using a suitably hydrophobic stabilizer block such as poly(lauryl methacrylate) or poly(stearyl methacrylate) should enable the formation of the analogous *water-in-oil* Pickering nanoemulsions if an *n*-alkane-insoluble core-forming block such as

PBzMA<sup>158</sup> or PTFEMA<sup>241</sup> confers sufficient stability to prevent *in situ* degradation during microfluidization. Indeed, we have just exemplified this concept.<sup>242</sup> Remarkably, PISA has also enabled the preparation of transparent Pickering double emulsions.<sup>191</sup> More specifically, the refractive index of the nanoparticle emulsifier can be tuned by selecting an appropriate core-forming block to match that of the chosen oil, with the refractive index of the aqueous phase being subsequently tuned by addition of a suitable water-soluble additive (e.g. sucrose or glycerol). Such studies highlight the rational design capability afforded by PISA for the preparation of a wide range of block copolymer nanoparticles to act as bespoke Pickering emulsifiers. This versatility augurs well for potential commercial applications of this technology.

## ACKNOWLEDGMENTS

EPSRC is thanked for a CDT PhD studentship to support S.J.H. (EP/L016281) and also an Established Career Particle Technology Fellowship (EP/R003009) for S.P.A. DSM (Geleen, The Netherlands) is acknowledged for partial support of S.J.H.'s PhD studentship and for permission to publish this work.

## REFERENCES

1. Ramsden, W., Separation of Solids in the Surface-Layers of Solutions and 'Suspensions' (Observations on Surface-Membranes, Bubbles, Emulsions, and Mechanical Coagulation). -- Preliminary Account. *Proc. R. Soc. London* **1903**, *72*, 156-164.
2. Pickering, S. U., Emulsions. *J. Chem. Soc.* **1907**, *91*, 2001-2021.
3. P. Binks, B.; O. Lumsdon, S., Stability of oil-in-water emulsions stabilised by silica particles. *Phys. Chem. Chem. Phys.* **1999**, *1*, 3007-3016.
4. Ashby, N. P.; Binks, B. P., Pickering emulsions stabilised by Laponite clay particles. *Phys. Chem. Chem. Phys.* **2000**, *2*, 5640-5646.
5. Binks, B. P.; Lumsdon, S. O., Influence of Particle Wettability on the Type and Stability of Surfactant-Free Emulsions. *Langmuir* **2000**, *16*, 8622-8631.
6. Binks, B. P., Particles as surfactants—similarities and differences. *Curr. Opin. Colloid Interface Sci.* **2002**, *7*, 21-41.
7. Aveyard, R.; Binks, B. P.; Clint, J. H., Emulsions stabilised solely by colloidal particles. *Adv. Colloid Interface Sci.* **2003**, *100*, 503-546.
8. Binks, B. P., Colloidal Particles at a Range of Fluid–Fluid Interfaces. *Langmuir* **2017**, *33*, 6947-6963.

9. Wu, J.; Shi, M.; Li, W.; Zhao, L.; Wang, Z.; Yan, X.; Norde, W.; Li, Y., Pickering emulsions stabilized by whey protein nanoparticles prepared by thermal cross-linking. *Colloids and Surfaces B: Biointerfaces* **2015**, *127*, 96-104.
10. Xiao, J.; Li, Y.; Huang, Q., Recent advances on food-grade particles stabilized Pickering emulsions: Fabrication, characterization and research trends. *Trends in Food Science & Technology* **2016**, *55*, 48-60.
11. Liu, F.; Tang, C.-H., Soy Protein Nanoparticle Aggregates as Pickering Stabilizers for Oil-in-Water Emulsions. *J Agr Food Chem* **2013**, *61*, 8888-8898.
12. Tang, C.; Li, Y.; Pun, J.; Mohamed Osman, A. S.; Tam, K. C., Polydopamine microcapsules from cellulose nanocrystal stabilized Pickering emulsions for essential oil and pesticide encapsulation. *Colloids Surf., A* **2019**, *570*, 403-413.
13. Fowler, J.; Pickering Emulsion Formulations, US Pat., 0234230, 2010.
14. Formstone, C., De Heer, M. I., Taylor, P. Haseldine, S. J.; Herbicidal Composition Comprising Polymeric Microparticles Containing a Herbicide, WO2013034513 A2, 2013.
15. Mulqueen, P. J., Taylor, P., Gittins, D. I.; Microencapsulation, WO2009063257 A2, 2009.
16. Marku, D.; Wahlgren, M.; Rayner, M.; Sjöo, M.; Timgren, A., Characterization of starch Pickering emulsions for potential applications in topical formulations. *Int J Pharm* **2012**, *428*, 1-7.
17. Marto, J.; Ascenso, A.; Simoes, S.; Almeida, A. J.; Ribeiro, H. M., Pickering emulsions: challenges and opportunities in topical delivery. *Expert Opinion on Drug Delivery* **2016**, *13*, 1093-1107.
18. Yang, Y.; Fang, Z.; Chen, X.; Zhang, W.; Xie, Y.; Chen, Y.; Liu, Z.; Yuan, W., An Overview of Pickering Emulsions: Solid-Particle Materials, Classification, Morphology, and Applications. *Frontiers in Pharmacology* **2017**, *8*.
19. Frelichowska, J.; Bolzinger, M.-A.; Valour, J.-P.; Mouaziz, H.; Pelletier, J.; Chevalier, Y., Pickering w/o emulsions: Drug release and topical delivery. *Int J Pharm* **2009**, *368*, 7-15.
20. Frelichowska, J.; Bolzinger, M.-A.; Pelletier, J.; Valour, J.-P.; Chevalier, Y., Topical delivery of lipophilic drugs from o/w Pickering emulsions. *Int J Pharm* **2009**, *371*, 56-63.
21. Finkle, P.; Draper, H. D.; Hildebrand, J. H., THE THEORY OF EMULSIFICATION1. *J. Am. Chem. Soc.* **1923**, *45*, 2780-2788.
22. Binks, B. P.; Lumsdon, S. O., Pickering Emulsions Stabilized by Monodisperse Latex Particles: Effects of Particle Size. *Langmuir* **2001**, *17*, 4540-4547.
23. Anjali, T. G.; Basavaraj, M. G., Shape-Anisotropic Colloids at Interfaces. *Langmuir* **2019**, *35*, 3-20.
24. Wilde, P., Interfaces: Their role in foam and emulsion behaviour. *Current Opinion in Colloid & Interface Science - CURR OPIN COLLOID INTERFACE S* **2000**, *5*, 176-181.
25. Kabalnov, A., Thermodynamic and theoretical aspects of emulsions and their stability. *Curr. Opin. Colloid Interface Sci.* **1998**, *3*, 270-275.
26. Levine, S.; Bowen, B. D.; Partridge, S. J., Stabilization of emulsions by fine particles I. Partitioning of particles between continuous phase and oil/water interface. *Colloids Surf.* **1989**, *38*, 325-343.
27. Clint, J. H.; Taylor, S. E., Particle size and interparticle forces of overbased detergents: A Langmuir trough study. *Colloids Surf.* **1992**, *65*, 61-67.
28. Garti, N., Double emulsions — scope, limitations and new achievements. *Colloids Surf., A* **1997**, *123-124*, 233-246.
29. Cunha, A. G.; Mougél, J.-B.; Cathala, B.; Berglund, L. A.; Capron, I., Preparation of Double Pickering Emulsions Stabilized by Chemically Tailored Nanocelluloses. *Langmuir* **2014**, *30*, 9327-9335.
30. Binks, B. P.; Lumsdon, S. O., Catastrophic Phase Inversion of Water-in-Oil Emulsions Stabilized by Hydrophobic Silica. *Langmuir* **2000**, *16*, 2539-2547.
31. Menner, A.; Ikem, V.; Salgueiro, M.; Shaffer, M. S. P.; Bismarck, A., High internal phase emulsion templates solely stabilised by functionalised titania nanoparticles. *Chem. Commun.* **2007**, 4274-4276.
32. Ikem, V. O.; Menner, A.; Bismarck, A., High-Porosity Macroporous Polymers Synthesized from Titania-Particle-Stabilized Medium and High Internal Phase Emulsions. *Langmuir* **2010**, *26*, 8836-8841.

33. Zhou, J.; Qiao, X.; Binks, B. P.; Sun, K.; Bai, M.; Li, Y.; Liu, Y., Magnetic Pickering Emulsions Stabilized by Fe<sub>3</sub>O<sub>4</sub> Nanoparticles. *Langmuir* **2011**, *27*, 3308-3316.
34. Binks, B. P.; Whitby, C. P., Nanoparticle silica-stabilised oil-in-water emulsions: improving emulsion stability. *Colloids Surf., A* **2005**, *253*, 105-115.
35. Frelichowska, J.; Bolzinger, M.-A.; Chevalier, Y., Pickering emulsions with bare silica. *Colloids Surf. A* **2009**, *343*, 70-74.
36. Tcholakova, S.; Denkov, N. D.; Lips, A., Comparison of solid particles, globular proteins and surfactants as emulsifiers. *Phys. Chem. Chem. Phys.* **2008**, *10*, 1608-1627.
37. Yang, F.; Liu, S.; Xu, J.; Lan, Q.; Wei, F.; Sun, D., Pickering emulsions stabilized solely by layered double hydroxides particles: The effect of salt on emulsion formation and stability. *J. Colloid Interface Sci.* **2006**, *302*, 159-169.
38. Kalashnikova, I.; Bizot, H.; Cathala, B.; Capron, I., New Pickering Emulsions Stabilized by Bacterial Cellulose Nanocrystals. *Langmuir* **2011**, *27*, 7471-7479.
39. Kalashnikova, I.; Bizot, H.; Bertoncini, P.; Cathala, B.; Capron, I., Cellulosic nanorods of various aspect ratios for oil in water Pickering emulsions. *Soft Matter* **2013**, *9*, 952-959.
40. Jiménez Saelices, C.; Capron, I., Design of Pickering Micro- and Nanoemulsions Based on the Structural Characteristics of Nanocelluloses. *Biomacromolecules* **2018**, *19*, 460-469.
41. Capron, I.; Rojas, O. J.; Bordes, R., Behavior of nanocelluloses at interfaces. *Curr. Opin. Colloid Interface Sci.* **2017**, *29*, 83-95.
42. Saha, A.; Nikova, A.; Venkataraman, P.; John, V. T.; Bose, A., Oil Emulsification Using Surface-Tunable Carbon Black Particles. *ACS Applied Materials & Interfaces* **2013**, *5*, 3094-3100.
43. Katepalli, H.; John, V. T.; Bose, A., The Response of Carbon Black Stabilized Oil-in-Water Emulsions to the Addition of Surfactant Solutions. *Langmuir* **2013**, *29*, 6790-6797.
44. Briggs, N. M.; Weston, J. S.; Li, B.; Venkataramani, D.; Aichele, C. P.; Harwell, J. H.; Crossley, S. P., Multiwalled Carbon Nanotubes at the Interface of Pickering Emulsions. *Langmuir* **2015**, *31*, 13077-13084.
45. He, Y. Q.; Wu, F.; Sun, X. Y.; Li, R. Q.; Guo, Y. Q.; Li, C. B.; Zhang, L.; Xing, F. B.; Wang, W.; Gao, J. P., Factors that Affect Pickering Emulsions Stabilized by Graphene Oxide. *Acs Applied Materials & Interfaces* **2013**, *5*, 4843-4855.
46. Kim, J.; Cote, L. J.; Kim, F.; Yuan, W.; Shull, K. R.; Huang, J. X., Graphene Oxide Sheets at Interfaces. *J. Am. Chem. Soc.* **2010**, *132*, 8180-8186.
47. Velev, O. D.; Furusawa, K.; Nagayama, K., Assembly of Latex Particles by Using Emulsion Droplets as Templates. 1. Microstructured Hollow Spheres. *Langmuir* **1996**, *12*, 2374-2384.
48. Dinsmore, A. D.; Hsu, M. F.; Nikolaidis, M. G.; Marquez, M.; Bausch, A. R.; Weitz, D. A., Colloidosomes: Selectively Permeable Capsules Composed of Colloidal Particles. *Science* **2002**, *298*, 1006-1009.
49. Amalvy, J. I.; Armes, S. P.; Binks, B. P.; Rodrigues, J. A.; Unali, G. F., Use of sterically-stabilised polystyrene latex particles as a pH-responsive particulate emulsifier to prepare surfactant-free oil-in-water emulsions. *Chem. Commun.* **2003**, 1826-1827.
50. Amalvy, J. I.; Unali, G. F.; Li, Y.; Granger-Bevan, S.; Armes, S. P.; Binks, B. P.; Rodrigues, J. A.; Whitby, C. P., Synthesis of Sterically Stabilized Polystyrene Latex Particles Using Cationic Block Copolymers and Macromonomers and Their Application as Stimulus-Responsive Particulate Emulsifiers for Oil-in-Water Emulsions. *Langmuir* **2004**, *20*, 4345-4354.
51. Binks, B. P.; Murakami, R.; Armes, S. P.; Fujii, S., Temperature-Induced Inversion of Nanoparticle-Stabilized Emulsions. *Angew. Chem.* **2005**, *117*, 4873-4876.
52. Binks, B. P.; Murakami, R.; Armes, S. P.; Fujii, S.; Schmid, A., pH-Responsive Aqueous Foams Stabilized by Ionizable Latex Particles. *Langmuir* **2007**, *23*, 8691-8694.
53. Fujii, S.; Cai, Y.; Weaver, J. V. M.; Armes, S. P., Syntheses of Shell Cross-Linked Micelles Using Acidic ABC Triblock Copolymers and Their Application as pH-Responsive Particulate Emulsifiers. *J. Am. Chem. Soc.* **2005**, *127*, 7304-7305.
54. Coertjens, S.; De Dier, R.; Moldenaers, P.; Isa, L.; Vermant, J., Adsorption of Ellipsoidal Particles at Liquid-Liquid Interfaces. *Langmuir* **2017**, *33*, 2689-2697.
55. Ngai, T.; Behrens, S. H.; Auweter, H., Novel emulsions stabilized by pH and temperature sensitive microgels. *Chem. Commun.* **2005**, 331-333.

56. Brugger, B.; Rosen, B. A.; Richtering, W., Microgels as Stimuli-Responsive Stabilizers for Emulsions. *Langmuir* **2008**, *24*, 12202-12208.
57. Wang, F.; Tang, J.; Liu, H.; Yu, G.; Zou, Y., Self-assembled polymeric micelles as amphiphilic particulate emulsifiers for controllable Pickering emulsions. *Materials Chemistry Frontiers* **2019**, *3*, 356-364.
58. Binks, B. P.; Whitby, C. P., Silica Particle-Stabilized Emulsions of Silicone Oil and Water: Aspects of Emulsification. *Langmuir* **2004**, *20*, 1130-1137.
59. Horozov, T. S.; Binks, B. P., Particle-Stabilized Emulsions: A Bilayer or a Bridging Monolayer? *Angew. Chem. Int. Ed.* **2006**, *45*, 773-776.
60. Fielding, L. A.; Armes, S. P., Preparation of Pickering emulsions and colloidosomes using either a glycerol-functionalised silica sol or core-shell polymer/silica nanocomposite particles. *J. Mater. Chem.* **2012**, *22*, 11235-11244.
61. Binks, B. P.; Rodrigues, J. A.; Frith, W. J., Synergistic Interaction in Emulsions Stabilized by a Mixture of Silica Nanoparticles and Cationic Surfactant. *Langmuir* **2007**, *23*, 3626-3636.
62. Binks, B. P.; Isa, L.; Tyowua, A. T., Direct Measurement of Contact Angles of Silica Particles in Relation to Double Inversion of Pickering Emulsions. *Langmuir* **2013**, *29*, 4923-4927.
63. Fouilloux, S.; Malloggi, F.; Daillant, J.; Thill, A., Aging mechanism in model Pickering emulsion. *Soft Matter* **2016**, *12*, 900-904.
64. Liu, K.; Jiang, J.; Cui, Z.; Binks, B. P., pH-Responsive Pickering Emulsions Stabilized by Silica Nanoparticles in Combination with a Conventional Zwitterionic Surfactant. *Langmuir* **2017**, *33*, 2296-2305.
65. Pieranski, P., Two-Dimensional Interfacial Colloidal Crystals. *Phys Rev Lett* **1980**, *45*, 569-572.
66. Binks, B. P.; Rodrigues, J. A., Enhanced Stabilization of Emulsions Due to Surfactant-Induced Nanoparticle Flocculation. *Langmuir* **2007**, *23*, 7436-7439.
67. Arditty, S.; Whitby, C. P.; Binks, B. P.; Schmitt, V.; Leal-Calderon, F., Some general features of limited coalescence in solid-stabilized emulsions. *The European Physical Journal E* **2003**, *11*, 273-281.
68. Dupin, D.; Armes, S. P.; Connan, C.; Reeve, P.; Baxter, S. M., How Does the Nature of the Steric Stabilizer Affect the Pickering Emulsifier Performance of Lightly Cross-Linked, Acid-Swellable Poly(2-vinylpyridine) Latexes? *Langmuir* **2007**, *23*, 6903-6910.
69. Guo, H.; Yang, D.; Yang, M.; Gao, Y.; Liu, Y.; Li, H., Dual responsive Pickering emulsions stabilized by constructed core crosslinked polymer nanoparticles via reversible covalent bonds. *Soft Matter* **2016**, *12*, 9683-9691.
70. Walsh, A.; Thompson, K. L.; Armes, S. P.; York, D. W., Polyamine-Functional Sterically Stabilized Latexes for Covalently Cross-Linkable Colloidosomes. In *Langmuir*, American Chemical Society: 2010; Vol. 26, pp 18039-18048.
71. Thompson, K. L.; Lane, J. A.; Derry, M. J.; Armes, S. P., Non-aqueous Isorefractive Pickering Emulsions. *Langmuir* **2015**, *31*, 4373-4376.
72. Mable, C. J.; Warren, N. J.; Thompson, K. L.; Mykhaylyk, O. O.; Armes, S. P., Framboidal ABC triblock copolymer vesicles: a new class of efficient Pickering emulsifier. *Chem. Sci.* **2015**, *6*, 6179-6188.
73. Thompson, K. L.; Mable, C. J.; Lane, J. A.; Derry, M. J.; Fielding, L. A.; Armes, S. P., Preparation of Pickering Double Emulsions Using Block Copolymer Worms. *Langmuir* **2015**, *31*, 4137-4144.
74. Rizzelli, S. L.; Jones, E. R.; Thompson, K. L.; Armes, S. P., Preparation of non-aqueous Pickering emulsions using anisotropic block copolymer nanoparticles. *Colloid. Polym. Sci.* **2016**, *294*, 1-12.
75. Read, E. S.; Fujii, S.; Amalvy, J. I.; Randall, D. P.; Armes, S. P., Effect of Varying the Oil Phase on the Behavior of pH-Responsive Latex-Based Emulsifiers: Demulsification versus Transitional Phase Inversion *Langmuir* **2005**, *21*, 1662-1662.
76. Fujii, S.; Read, E. S.; Binks, B. P.; Armes, S. P., Stimulus-Responsive Emulsifiers Based on Nanocomposite Microgel Particles. *Adv. Mater.* **2005**, *17*, 1014-1018.

77. Fujii, S.; Armes, S. P.; Binks, B. P.; Murakami, R., Stimulus-Responsive Particulate Emulsifiers Based on Lightly Cross-Linked Poly(4-vinylpyridine)–Silica Nanocomposite Microgels. *Langmuir* **2006**, *22*, 6818-6825.
78. Morse, A. J.; Dupin, D.; Thompson, K. L.; Armes, S. P.; Ouzineb, K.; Mills, P.; Swart, R., Novel Pickering Emulsifiers based on pH-Responsive Poly(tert-butylaminoethyl methacrylate) Latexes. *Langmuir* **2012**, *28*, 11733-11744.
79. Morse, A. J.; Armes, S. P.; Thompson, K. L.; Dupin, D.; Fielding, L. A.; Mills, P.; Swart, R., Novel Pickering Emulsifiers Based on pH-Responsive Poly(2-(diethylamino)ethyl methacrylate) Latexes. *Langmuir* **2013**, *29*, 5466-5475.
80. Ngai, T.; Auweter, H.; Behrens, S. H., Environmental Responsiveness of Microgel Particles and Particle-Stabilized Emulsions. *Macromolecules* **2006**, *39*, 8171-8177.
81. Brugger, B.; Rütten, S.; Phan, K.-H.; Möller, M.; Richtering, W., The Colloidal Suprastructure of Smart Microgels at Oil–Water Interfaces. *Angew. Chem. Int. Ed.* **2009**, *48*, 3978-3981.
82. Schild, H. G., Poly(N-isopropylacrylamide): experiment, theory and application. *Progress in Polymer Science* **1992**, *17*, 163-249.
83. Pelton, R. H.; Chibante, P., Preparation of aqueous latices with N-isopropylacrylamide. *Colloids Surf.* **1986**, *20*, 247-256.
84. Pelton, R., Temperature-sensitive aqueous microgels. *Adv. Colloid Interface Sci.* **2000**, *85*, 1-33.
85. Snowden, M. J.; Chowdhry, B. Z.; Vincent, B.; Morris, G. E., Colloidal copolymer microgels of N-isopropylacrylamide and acrylic acid: pH, ionic strength and temperature effects. *Journal of the Chemical Society, Faraday Transactions* **1996**, *92*, 5013-5016.
86. Tsuji, S.; Kawaguchi, H., Thermosensitive Pickering Emulsion Stabilized by Poly(N-isopropylacrylamide)-Carrying Particles. *Langmuir* **2008**, *24*, 3300-3305.
87. Brugger, B.; Richtering, W., Emulsions Stabilized by Stimuli-Sensitive Poly(N-isopropylacrylamide)-co-Methacrylic Acid Polymers: Microgels versus Low Molecular Weight Polymers. *Langmuir* **2008**, *24*, 7769-7777.
88. Brugger, B.; Vermant, J.; Richtering, W., Interfacial layers of stimuli-responsive poly-(N-isopropylacrylamide-co-methacrylic acid) (PNIPAM-co-MAA) microgels characterized by interfacial rheology and compression isotherms. *Phys. Chem. Chem. Phys.* **2010**, *12*, 14573-14578.
89. Richtering, W., Responsive Emulsions Stabilized by Stimuli-Sensitive Microgels: Emulsions with Special Non-Pickering Properties. *Langmuir* **2012**, *28*, 17218-17229.
90. Geisel, K.; Isa, L.; Richtering, W., Unraveling the 3D Localization and Deformation of Responsive Microgels at Oil/Water Interfaces: A Step Forward in Understanding Soft Emulsion Stabilizers. *Langmuir* **2012**, *28*, 15770-15776.
91. Szwarc, M., 'Living' Polymers. *Nature* **1956**, *178*, 1168-1169.
92. Szwarc, M.; Levy, M.; Milkovich, R., Polymerization Initiated by Electron Transfer to Monomer. A New Method of Formation of Block Copolymers. *J. Am. Chem. Soc.* **1956**, *78*, 2656-2657.
93. Gao, Z.; Varshney, S. K.; Wong, S.; Eisenberg, A., Block Copolymer "Crew-Cut" Micelles in Water. *Macromolecules* **1994**, *27*, 7923-7927.
94. Zhang, L.; Eisenberg, A., Multiple Morphologies of "Crew-Cut" Aggregates of Polystyrene-b-poly(acrylic acid) Block Copolymers. *Science* **1995**, *268*, 1728-1731.
95. Zhang, L.; Eisenberg, A., Multiple Morphologies and Characteristics of "Crew-Cut" Micelle-like Aggregates of Polystyrene-b-poly(acrylic acid) Diblock Copolymers in Aqueous Solutions. *J. Am. Chem. Soc.* **1996**, *118*, 3168-3181.
96. Discher, B. M.; Won, Y.-Y.; Ege, D. S.; Lee, J. C.-M.; Bates, F. S.; Discher, D. E.; Hammer, D. A., Polymersomes: Tough Vesicles Made from Diblock Copolymers. *Science* **1999**, *284*, 1143-1146.
97. Mai, Y.; Eisenberg, A., Self-assembly of block copolymers. *Chem. Soc. Rev.* **2012**, *41*, 5969-5985.
98. Matsen, M. W.; Bates, F. S., Origins of Complex Self-Assembly in Block Copolymers. *Macromolecules* **1996**, *29*, 7641-7644.

99. Patten, T. E.; Matyjaszewski, K., Atom Transfer Radical Polymerization and the Synthesis of Polymeric Materials. *Adv. Mater.* **1998**, *10*, 901-915.
100. Hawker, C. J.; Bosman, A. W.; Harth, E., New Polymer Synthesis by Nitroxide Mediated Living Radical Polymerizations. *Chem. Rev.* **2001**, *101*, 3661-3688.
101. Moad, G.; Rizzardo, E.; Thang, S. H., Living Radical Polymerization by the RAFT Process. *Aust. J. Chem.* **2005**, *58*, 379-410.
102. Chiefari, J.; Chong, Y. K.; Ercole, F.; Krstina, J.; Jeffery, J.; Le, T. P. T.; Mayadunne, R. T. A.; Meijs, G. F.; Moad, C. L.; Moad, G.; Rizzardo, E.; Thang, S. H., Living Free-Radical Polymerization by Reversible Addition-Fragmentation Chain Transfer: The RAFT Process. *Macromolecules* **1998**, *31*, 5559-5562.
103. Moad, G.; Rizzardo, E.; Thang, S. H., Living Radical Polymerization by the RAFT Process A First Update. *Aust. J. Chem.* **2006**, *59*, 669-692.
104. Moad, G.; Rizzardo, E.; Thang, S. H., Living Radical Polymerization by the RAFT Process – A Second Update. *Aust. J. Chem.* **2009**, *62*, 1402-1472.
105. Moad, G.; Rizzardo, E.; Thang, S. H., Living Radical Polymerization by the RAFT Process – A Third Update. *Aust. J. Chem.* **2012**, *65*, 985-1076.
106. Mühlebach, A.; Gaynor, S. G.; Matyjaszewski, K., Synthesis of Amphiphilic Block Copolymers by Atom Transfer Radical Polymerization (ATRP). *Macromolecules* **1998**, *31*, 6046-6052.
107. Delaittre, G.; Nicolas, J.; Lefay, C.; Save, M.; Charleux, B., Surfactant-free synthesis of amphiphilic diblock copolymer nanoparticles via nitroxide-mediated emulsion polymerization. *Chem. Commun.* **2005**, 614-616.
108. Ferguson, C. J.; Hughes, R. J.; Pham, B. T. T.; Hawckett, B. S.; Gilbert, R. G.; Serelis, A. K.; Such, C. H., Effective *ab Initio* Emulsion Polymerization under RAFT Control. *Macromolecules* **2002**, *35*, 9243-9245.
109. Warren, N. J.; Armes, S. P., Polymerization-Induced Self-Assembly of Block Copolymer Nano-objects via RAFT Aqueous Dispersion Polymerization. *J. Am. Chem. Soc.* **2014**, *136*, 10174-10185.
110. Derry, M. J.; Fielding, L. A.; Armes, S. P., Polymerization-induced self-assembly of block copolymer nanoparticles via RAFT non-aqueous dispersion polymerization. *Progress in Polymer Science* **2016**, *52*, 1-18.
111. Canning, S. L.; Smith, G. N.; Armes, S. P., A Critical Appraisal of RAFT-Mediated Polymerization-Induced Self-Assembly. *Macromolecules* **2016**, *49*, 1985-2001.
112. Penfold, N. J. W.; Yeow, J.; Boyer, C.; Armes, S. P., Emerging Trends in Polymerization-Induced Self-Assembly. *ACS Macro Lett.* **2019**, *8*, 1029-1054.
113. D'Agosto, F.; Rieger, J.; Lansalot, M., RAFT-Mediated Polymerization-Induced Self-Assembly. *Angew. Chem. Int. Ed. n/a*.
114. Rieger, J., Guidelines for the Synthesis of Block Copolymer Particles of Various Morphologies by RAFT Dispersion Polymerization. *Macromol. Rapid Commun.* **2015**, *36*, 1458-1471.
115. Charleux, B.; Delaittre, G.; Rieger, J.; D'Agosto, F., Polymerization-Induced Self-Assembly: From Soluble Macromolecules to Block Copolymer Nano-Objects in One Step. *Macromolecules* **2012**, *45*, 6753-6765.
116. Derry, M. J.; Fielding, L. A.; Armes, S. P., Industrially-relevant polymerization-induced self-assembly formulations in non-polar solvents: RAFT dispersion polymerization of benzyl methacrylate. *Polym. Chem.* **2015**, *6*, 3054-3062.
117. Cunningham, V. J.; Alswieleh, A. M.; Thompson, K. L.; Williams, M.; Leggett, G. J.; Armes, S. P.; Musa, O. M., Poly(glycerol monomethacrylate)-Poly(benzyl methacrylate) Diblock Copolymer Nanoparticles via RAFT Emulsion Polymerization: Synthesis, Characterization, and Interfacial Activity. *Macromolecules* **2014**, *47*, 5613-5623.
118. Prescott, S. W.; Ballard, M. J.; Rizzardo, E.; Gilbert, R. G., RAFT in Emulsion Polymerization: What Makes it Different? *Aust. J. Chem.* **2002**, *55*, 415-424.
119. Prescott, S. W.; Ballard, M. J.; Rizzardo, E.; Gilbert, R. G., Rate Optimization in Controlled Radical Emulsion Polymerization Using RAFT. *Macromolecular Theory and Simulations* **2006**, *15*, 70-86.

120. Ferguson, C. J.; Hughes, R. J.; Nguyen, D.; Pham, B. T. T.; Gilbert, R. G.; Serelis, A. K.; Such, C. H.; Hawckett, B. S., Ab Initio Emulsion Polymerization by RAFT-Controlled Self-Assembly. *Macromolecules* **2005**, *38*, 2191-2204.
121. Truong, N. P.; Dussert, M. V.; Whittaker, M. R.; Quinn, J. F.; Davis, T. P., Rapid synthesis of ultrahigh molecular weight and low polydispersity polystyrene diblock copolymers by RAFT-mediated emulsion polymerization. *Polym. Chem.* **2015**, *6*, 3865-3874.
122. Ganeva, D. E.; Sprong, E.; de Bruyn, H.; Warr, G. G.; Such, C. H.; Hawckett, B. S., Particle Formation in ab Initio RAFT Mediated Emulsion Polymerization Systems. *Macromolecules* **2007**, *40*, 6181-6189.
123. Chaduc, I.; Crepet, A.; Boyron, O.; Charleux, B.; D'Agosto, F.; Lansalot, M., Effect of the pH on the RAFT Polymerization of Acrylic Acid in Water. Application to the Synthesis of Poly(acrylic acid)-Stabilized Polystyrene Particles by RAFT Emulsion Polymerization. *Macromolecules* **2013**, *46*, 6013-6023.
124. Chaduc, I.; Zhang, W.; Rieger, J.; Lansalot, M.; D'Agosto, F.; Charleux, B., Amphiphilic Block Copolymers from a Direct and One-pot RAFT Synthesis in Water. *Macromol. Rapid Commun.* **2011**, *32*, 1270-1276.
125. Chaduc, I.; Girod, M.; Antoine, R.; Charleux, B.; D'Agosto, F.; Lansalot, M., Batch Emulsion Polymerization Mediated by Poly(methacrylic acid) MacroRAFT Agents: One-Pot Synthesis of Self-Stabilized Particles. *Macromolecules* **2012**, *45*, 5881-5893.
126. Poon, C. K.; Tang, O.; Chen, X.-M.; Pham, B. T. T.; Gody, G.; Pollock, C. A.; Hawckett, B. S.; Perrier, S., Preparation of Inert Polystyrene Latex Particles as MicroRNA Delivery Vectors by Surfactant-Free RAFT Emulsion Polymerization. *Biomacromolecules* **2016**, *17*, 965-973.
127. Rieger, J.; Stoffelbach, F.; Bui, C.; Alaimo, D.; Jérôme, C.; Charleux, B., Amphiphilic Poly(ethylene oxide) Macromolecular RAFT Agent as a Stabilizer and Control Agent in ab Initio Batch Emulsion Polymerization. *Macromolecules* **2008**, *41*, 4065-4068.
128. Rieger, J.; Zhang, W.; Stoffelbach, F.; Charleux, B., Surfactant-Free RAFT Emulsion Polymerization Using Poly(N,N-dimethylacrylamide) Trithiocarbonate Macromolecular Chain Transfer Agents. *Macromolecules* **2010**, *43*, 6302-6310.
129. Rieger, J.; Osterwinter, G.; Bui, C.; Stoffelbach, F.; Charleux, B., Surfactant-Free Controlled/Living Radical Emulsion (Co)polymerization of n-Butyl Acrylate and Methyl Methacrylate via RAFT Using Amphiphilic Poly(ethylene oxide)-Based Trithiocarbonate Chain Transfer Agents. *Macromolecules* **2009**, *42*, 5518-5525.
130. Boissé, S.; Rieger, J.; Pembouong, G.; Beaunier, P.; Charleux, B., Influence of the stirring speed and CaCl<sub>2</sub> concentration on the nano-object morphologies obtained via RAFT-mediated aqueous emulsion polymerization in the presence of a water-soluble macroRAFT agent. *J. Polym. Sci., Part A: Polym. Chem.* **2011**, *49*, 3346-3354.
131. Zhang, W.; D'Agosto, F.; Boyron, O.; Rieger, J.; Charleux, B., One-Pot Synthesis of Poly(methacrylic acid-co-poly(ethylene oxide) methyl ether methacrylate)-b-polystyrene Amphiphilic Block Copolymers and Their Self-Assemblies in Water via RAFT-Mediated Radical Emulsion Polymerization. A Kinetic Study. *Macromolecules* **2011**, *44*, 7584-7593.
132. Grazon, C.; Rieger, J.; Sanson, N.; Charleux, B., Study of poly(N,N-diethylacrylamide) nanogel formation by aqueous dispersion polymerization of N,N-diethylacrylamide in the presence of poly(ethylene oxide)-b-poly(N,N-dimethylacrylamide) amphiphilic macromolecular RAFT agents. *Soft Matter* **2011**, *7*, 3482-3490.
133. Zhang, W.; D'Agosto, F.; Boyron, O.; Rieger, J.; Charleux, B., Toward a Better Understanding of the Parameters that Lead to the Formation of Nonspherical Polystyrene Particles via RAFT-Mediated One-Pot Aqueous Emulsion Polymerization. *Macromolecules* **2012**, *45*, 4075-4084.
134. Zhang, W.; D'Agosto, F.; Dugas, P.-Y.; Rieger, J.; Charleux, B., RAFT-mediated one-pot aqueous emulsion polymerization of methyl methacrylate in presence of poly(methacrylic acid-co-poly(ethylene oxide) methacrylate) trithiocarbonate macromolecular chain transfer agent. *Polymer* **2013**, *54*, 2011-2019.
135. Canton, I.; Warren, N. J.; Chahal, A.; Amps, K.; Wood, A.; Weightman, R.; Wang, E.; Moore, H.; Armes, S. P., Mucin-Inspired Thermoresponsive Synthetic Hydrogels Induce Stasis in Human Pluripotent Stem Cells and Human Embryos. *ACS Central Science* **2016**, *2*, 65-74.

136. Penfold, N. J. W.; Ning, Y.; Verstraete, P.; Smets, J.; Armes, S. P., Cross-linked cationic diblock copolymer worms are superflocculants for micrometer-sized silica particles. *Chem. Sci.* **2016**, *7*, 6894-6904.
137. Warren, N. J.; Mykhaylyk, O. O.; Mahmood, D.; Ryan, A. J.; Armes, S. P., RAFT Aqueous Dispersion Polymerization Yields Poly(ethylene glycol)-Based Diblock Copolymer Nano-Objects with Predictable Single Phase Morphologies. *J. Am. Chem. Soc.* **2014**, *136*, 1023-1033.
138. Blanazs, A.; Armes, S. P.; Ryan, A. J., Self-Assembled Block Copolymer Aggregates: From Micelles to Vesicles and their Biological Applications. *Macromol. Rapid Commun.* **2009**, *30*, 267-277.
139. Blanazs, A.; Madsen, J.; Battaglia, G.; Ryan, A. J.; Armes, S. P., Mechanistic Insights for Block Copolymer Morphologies: How Do Worms Form Vesicles? *J. Am. Chem. Soc.* **2011**, *133*, 16581-16587.
140. Blanazs, A.; Ryan, A. J.; Armes, S. P., Predictive Phase Diagrams for RAFT Aqueous Dispersion Polymerization: Effect of Block Copolymer Composition, Molecular Weight, and Copolymer Concentration. *Macromolecules* **2012**, *45*, 5099-5107.
141. Verber, R.; Blanazs, A.; Armes, S. P., Rheological studies of thermo-responsive diblock copolymer worm gels. *Soft Matter* **2012**, *8*, 9915-9922.
142. Jiang, Y.; Xu, N.; Han, J.; Yu, Q.; Guo, L.; Gao, P.; Lu, X.; Cai, Y., The direct synthesis of interface-decorated reactive block copolymer nanoparticles via polymerisation-induced self-assembly. *Polym. Chem.* **2015**, *6*, 4955-4965.
143. Shen, W.; Chang, Y.; Liu, G.; Wang, H.; Cao, A.; An, Z., Biocompatible, Antifouling, and Thermosensitive Core-Shell Nanogels Synthesized by RAFT Aqueous Dispersion Polymerization. *Macromolecules* **2011**, *44*, 2524-2530.
144. Semsarilar, M.; Jones, E. R.; Blanazs, A.; Armes, S. P., Efficient Synthesis of Sterically-Stabilized Nano-Objects via RAFT Dispersion Polymerization of Benzyl Methacrylate in Alcoholic Media. *Adv. Mater.* **2012**, *24*, 3378-3382.
145. Gonzato, C.; Semsarilar, M.; Jones, E. R.; Li, F.; Krooshof, G. J. P.; Wyman, P.; Mykhaylyk, O. O.; Tuinier, R.; Armes, S. P., Rational Synthesis of Low-Polydispersity Block Copolymer Vesicles in Concentrated Solution via Polymerization-Induced Self-Assembly. *J. Am. Chem. Soc.* **2014**, *136*, 11100-11106.
146. Jones, E. R.; Semsarilar, M.; Blanazs, A.; Armes, S. P., Efficient Synthesis of Amine-Functional Diblock Copolymer Nanoparticles via RAFT Dispersion Polymerization of Benzyl Methacrylate in Alcoholic Media. *Macromolecules* **2012**, *45*, 5091-5098.
147. Pei, Y.; Dharsana, N. C.; van Hensbergen, J. A.; Burford, R. P.; Roth, P. J.; Lowe, A. B., RAFT dispersion polymerization of 3-phenylpropyl methacrylate with poly[2-(dimethylamino)ethyl methacrylate] macro-CTAs in ethanol and associated thermoreversible polymorphism. *Soft Matter* **2014**, *10*, 5787-5796.
148. Jones, E. R.; Semsarilar, M.; Wyman, P.; Boerakker, M.; Armes, S. P., Addition of water to an alcoholic RAFT PISA formulation leads to faster kinetics but limits the evolution of copolymer morphology. *Polym. Chem.* **2016**, *7*, 851-859.
149. Gibson, R. R.; Cornel, E. J.; Musa, O. M.; Fernyhough, A.; Armes, S. P., RAFT dispersion polymerisation of lauryl methacrylate in ethanol-water binary mixtures: synthesis of diblock copolymer vesicles with deformable membranes. *Polym. Chem.* **2020**, *11*, 1785-1796.
150. Ding, Z.; Gao, C.; Wang, S.; Liu, H.; Zhang, W., Macro-RAFT agent mediated dispersion polymerization: the monomer concentration effect on the morphology of the in situ synthesized block copolymer nano-objects. *Polym. Chem.* **2015**, *6*, 8003-8011.
151. Zehm, D.; Ratcliffe, L. P. D.; Armes, S. P., Synthesis of Diblock Copolymer Nanoparticles via RAFT Alcoholic Dispersion Polymerization: Effect of Block Copolymer Composition, Molecular Weight, Copolymer Concentration, and Solvent Type on the Final Particle Morphology. *Macromolecules* **2013**, *46*, 128-139.
152. Lowe, A. B., RAFT alcoholic dispersion polymerization with polymerization-induced self-assembly. *Polymer* **2016**, *106*, 161-181.
153. Wan, W.-M.; Sun, X.-L.; Pan, C.-Y., Formation of Vesicular Morphologies via Polymerization Induced Self-Assembly and Re-Organization. *Macromol. Rapid Commun.* **2010**, *31*, 399-404.

154. Huang, C.-Q.; Pan, C.-Y., Direct preparation of vesicles from one-pot RAFT dispersion polymerization. *Polymer* **2010**, *51*, 5115-5121.
155. Huang, C.-Q.; Wang, Y.; Hong, C.-Y.; Pan, C.-Y., Spiropyran-Based Polymeric Vesicles: Preparation and Photochromic Properties. *Macromol. Rapid Commun.* **2011**, *32*, 1174-1179.
156. He, W.-D.; Sun, X.-L.; Wan, W.-M.; Pan, C.-Y., Multiple Morphologies of PAA-b-PSt Assemblies throughout RAFT Dispersion Polymerization of Styrene with PAA Macro-CTA. *Macromolecules* **2011**, *44*, 3358-3365.
157. Karagoz, B.; Boyer, C.; Davis, T. P., Simultaneous Polymerization-Induced Self-Assembly (PISA) and Guest Molecule Encapsulation. *Macromol. Rapid Commun.* **2014**, *35*, 417-421.
158. Fielding, L. A.; Derry, M. J.; Ladmiral, V.; Rosselgong, J.; Rodrigues, A. M.; Ratcliffe, L. P. D.; Sugihara, S.; Armes, S. P., RAFT dispersion polymerization in non-polar solvents: facile production of block copolymer spheres, worms and vesicles in n-alkanes. *Chem. Sci.* **2013**, *4*, 2081-2087.
159. Fielding, L. A.; Lane, J. A.; Derry, M. J.; Mykhaylyk, O. O.; Armes, S. P., Thermo-responsive Diblock Copolymer Worm Gels in Non-polar Solvents. *J. Am. Chem. Soc.* **2014**, *136*, 5790-5798.
160. Houillot, L.; Bui, C.; Save, M.; Charleux, B.; Farcet, C.; Moire, C.; Raust, J.-A.; Rodriguez, I., Synthesis of Well-Defined Polyacrylate Particle Dispersions in Organic Medium Using Simultaneous RAFT Polymerization and Self-Assembly of Block Copolymers. A Strong Influence of the Selected Thiocarbonylthio Chain Transfer Agent. *Macromolecules* **2007**, *40*, 6500-6509.
161. Pei, Y.; Thurairajah, L.; Sugita, O. R.; Lowe, A. B., RAFT Dispersion Polymerization in Nonpolar Media: Polymerization of 3-Phenylpropyl Methacrylate in n-Tetradecane with Poly(stearyl methacrylate) Homopolymers as Macro Chain Transfer Agents. *Macromolecules* **2015**, *48*, 236-244.
162. Lopez-Oliva, A. P.; Warren, N. J.; Rajkumar, A.; Mykhaylyk, O. O.; Derry, M. J.; Doncom, K. E. B.; Rymaruk, M. J.; Armes, S. P., Polydimethylsiloxane-Based Diblock Copolymer Nano-objects Prepared in Nonpolar Media via RAFT-Mediated Polymerization-Induced Self-Assembly. *Macromolecules* **2015**, *48*, 3547-3555.
163. Smith, G. N.; Canning, S. L.; Derry, M. J.; Jones, E. R.; Neal, T. J.; Smith, A. J., Ionic and Nonspherical Polymer Nanoparticles in Nonpolar Solvents. *Macromolecules* **2020**, *53*, 3148-3156.
164. Zhang, Q.; Zhu, S., Ionic Liquids: Versatile Media for Preparation of Vesicles from Polymerization-Induced Self-Assembly. *ACS Macro Lett.* **2015**, *4*, 755-758.
165. Rymaruk, M. J.; Hunter, S. J.; O'Brien, C. T.; Brown, S. L.; Williams, C. N.; Armes, S. P., RAFT Dispersion Polymerization in Silicone Oil. *Macromolecules* **2019**, *52*, 2822-2832.
166. Rymaruk, M. J.; O'Brien, C. T.; Brown, S. L.; Williams, C. N.; Armes, S. P., RAFT Dispersion Polymerization of Benzyl Methacrylate in Silicone Oil Using a Silicone-Based Methacrylic Stabilizer Provides Convenient Access to Spheres, Worms, and Vesicles. *Macromolecules* **2020**, *53*, 1785-1794.
167. Hasell, T.; Thurecht, K. J.; Jones, R. D. W.; Brown, P. D.; Howdle, S. M., Novel one pot synthesis of silver nanoparticle-polymer composites by supercritical CO<sub>2</sub> polymerisation in the presence of a RAFT agent. *Chem. Commun.* **2007**, 3933-3935.
168. Zong, M.; Thurecht, K. J.; Howdle, S. M., Dispersion polymerisation in supercritical CO<sub>2</sub> using macro-RAFT agents. *Chem. Commun.* **2008**, 5942-5944.
169. Dong, S.; Zhao, W.; Lucien, F. P.; Perrier, S.; Zetterlund, P. B., Polymerization induced self-assembly: tuning of nano-object morphology by use of CO<sub>2</sub>. *Polym. Chem.* **2015**, *6*, 2249-2254.
170. Xu, A.; Lu, Q.; Huo, Z.; Ma, J.; Geng, B.; Azhar, U.; Zhang, L.; Zhang, S., Synthesis of fluorinated nanoparticles via RAFT dispersion polymerization-induced self-assembly using fluorinated macro-RAFT agents in supercritical carbon dioxide. *RSC Advances* **2017**, *7*, 51612-51620.
171. Byard, S. J.; Williams, M.; McKenzie, B. E.; Blanazs, A.; Armes, S. P., Preparation and Cross-Linking of All-Acrylamide Diblock Copolymer Nano-Objects via Polymerization-Induced Self-Assembly in Aqueous Solution. *Macromolecules* **2017**, *50*, 1482-1493.
172. Penfold, N. J. W.; Whatley, J. R.; Armes, S. P., Thermoreversible Block Copolymer Worm Gels Using Binary Mixtures of PEG Stabilizer Blocks. *Macromolecules* **2019**, *52*, 1653-1662.
173. Byard, S. J.; O'Brien, C. T.; Derry, M. J.; Williams, M.; Mykhaylyk, O. O.; Blanazs, A.; Armes, S. P., Unique aqueous self-assembly behavior of a thermoresponsive diblock copolymer. *Chem. Sci.* **2020**, *11*, 396-402.

174. Zhang, B.; Lv, X.; Zhu, A.; Zheng, J.; Yang, Y.; An, Z., Morphological Stabilization of Block Copolymer Worms Using Asymmetric Cross-Linkers during Polymerization-Induced Self-Assembly. *Macromolecules* **2018**, *51*, 2776-2784.
175. Zhang, B.; Lv, X.; An, Z., Modular Monomers with Tunable Solubility: Synthesis of Highly Incompatible Block Copolymer Nano-Objects via RAFT Aqueous Dispersion Polymerization. *ACS Macro Lett.* **2017**, *6*, 224-228.
176. Blackman, L. D.; Doncom, K. E. B.; Gibson, M. I.; O'Reilly, R. K., Comparison of photo- and thermally initiated polymerization-induced self-assembly: a lack of end group fidelity drives the formation of higher order morphologies. *Polym. Chem.* **2017**, *8*, 2860-2871.
177. Qiu, L.; Zhang, H.; Wang, B.; Zhan, Y.; Xing, C.; Pan, C.-Y., CO<sub>2</sub>-Responsive Nano-Objects with Assembly-Related Aggregation-Induced Emission and Tunable Morphologies. *ACS Applied Materials & Interfaces* **2020**, *12*, 1348-1358.
178. Varlas, S.; Foster, J. C.; Georgiou, P. G.; Keogh, R.; Husband, J. T.; Williams, D. S.; O'Reilly, R. K., Tuning the membrane permeability of polymersome nanoreactors developed by aqueous emulsion polymerization-induced self-assembly. *Nanoscale* **2019**, *11*, 12643-12654.
179. Yao, H.; Ning, Y.; Jesson, C. P.; He, J.; Deng, R.; Tian, W.; Armes, S. P., Using Host-Guest Chemistry to Tune the Kinetics of Morphological Transitions Undertaken by Block Copolymer Vesicles. *ACS Macro Lett.* **2017**, *6*, 1379-1385.
180. Mable, C. J.; Fielding, L. A.; Derry, M. J.; Mykhaylyk, O. O.; Chambon, P.; Armes, S. P., Synthesis and pH-responsive dissociation of framboidal ABC triblock copolymer vesicles in aqueous solution. *Chem. Sci.* **2018**, *9*, 1454-1463.
181. Xu, Q.; Zhang, Y.; Li, X.; He, J.; Tan, J.; Zhang, L., Enzyme catalysis-induced RAFT polymerization in water for the preparation of epoxy-functionalized triblock copolymer vesicles. *Polym. Chem.* **2018**, *9*, 4908-4916.
182. Wang, X.; Zhou, J.; Lv, X.; Zhang, B.; An, Z., Temperature-Induced Morphological Transitions of Poly(dimethylacrylamide)-Poly(diacetone acrylamide) Block Copolymer Lamellae Synthesized via Aqueous Polymerization-Induced Self-Assembly. *Macromolecules* **2017**, *50*, 7222-7232.
183. Yang, P.; Ratcliffe, L. P. D.; Armes, S. P., Efficient Synthesis of Poly(methacrylic acid)-block-Poly(styrene-alt-N-phenylmaleimide) Diblock Copolymer Lamellae Using RAFT Dispersion Polymerization. *Macromolecules* **2013**, *46*, 8545-8556.
184. Yang, P.; Mykhaylyk, O. O.; Jones, E. R.; Armes, S. P., RAFT Dispersion Alternating Copolymerization of Styrene with N-Phenylmaleimide: Morphology Control and Application as an Aqueous Foam Stabilizer. *Macromolecules* **2016**, *49*, 6731-6742.
185. Israelachvili, J. N.; Mitchell, D. J.; Ninham, B. W., Theory of self-assembly of hydrocarbon amphiphiles into micelles and bilayers. *Journal of the Chemical Society, Transactions* **1976**, *72*, 1525-1568.
186. Chambon, P.; Blanazs, A.; Battaglia, G.; Armes, S. P., Facile Synthesis of Methacrylic ABC Triblock Copolymer Vesicles by RAFT Aqueous Dispersion Polymerization. *Macromolecules* **2012**, *45*, 5081-5090.
187. Thompson, K. L.; Chambon, P.; Verber, R.; Armes, S. P., Can Polymersomes Form Colloidosomes? *J. Am. Chem. Soc.* **2012**, *134*, 12450-12453.
188. Thompson, K. L.; Mable, C. J.; Cockram, A.; Warren, N. J.; Cunningham, V. J.; Jones, E. R.; Verber, R.; Armes, S. P., Are block copolymer worms more effective Pickering emulsifiers than block copolymer spheres? *Soft Matter* **2014**, *10*, 8615-8626.
189. Thompson, K. L.; Fielding, L. A.; Mykhaylyk, O. O.; Lane, J. A.; Derry, M. J.; Armes, S. P., Vermicious thermo-responsive Pickering emulsifiers. *Chem. Sci.* **2015**, *6*, 4207-4214.
190. Mable, C. J.; Thompson, K. L.; Derry, M. J.; Mykhaylyk, O. O.; Binks, B. P.; Armes, S. P., ABC Triblock Copolymer Worms: Synthesis, Characterization, and Evaluation as Pickering Emulsifiers for Millimeter-Sized Droplets. *Macromolecules* **2016**, *49*, 7897-7907.
191. Rymaruk, M. J.; Thompson, K. L.; Derry, M. J.; Warren, N. J.; Ratcliffe, L. P. D.; Williams, C. N.; Brown, S. L.; Armes, S. P., Bespoke contrast-matched diblock copolymer nanoparticles enable the rational design of highly transparent Pickering double emulsions. *Nanoscale* **2016**, *8*, 14497-14506.

192. Thompson, K. L.; Cinotti, N.; Jones, E. R.; Mable, C. J.; Fowler, P. W.; Armes, S. P., Bespoke Diblock Copolymer Nanoparticles Enable the Production of Relatively Stable Oil-in-Water Pickering Nanoemulsions. *Langmuir* **2017**, *33*, 12616-12623.
193. Thompson, K. L.; Derry, M. J.; Hatton, F. L.; Armes, S. P., Long-Term Stability of n-Alkane-in-Water Pickering Nanoemulsions: Effect of Aqueous Solubility of Droplet Phase on Ostwald Ripening. *Langmuir* **2018**, *34*, 9289-9297.
194. Hunter, S. J.; Thompson, K. L.; Lovett, J. R.; Hatton, F. L.; Derry, M. J.; Lindsay, C.; Taylor, P.; Armes, S. P., Synthesis, Characterization, and Pickering Emulsifier Performance of Anisotropic Cross-Linked Block Copolymer Worms: Effect of Aspect Ratio on Emulsion Stability in the Presence of Surfactant. *Langmuir* **2019**, *35*, 254-265.
195. Cunningham, V. J.; Giakoumatos, E. C.; Ireland, P. M.; Mable, C. J.; Armes, S. P.; Wanless, E. J., Giant Pickering Droplets: Effect of Nanoparticle Size and Morphology on Stability. *Langmuir* **2017**, *33*, 7669-7679.
196. Aveyard, R.; Binks, B. P.; Clint, J. H., Emulsions stabilised solely by colloidal particles. *Adv. Colloid Interface Sci.* **2003**, *100-102*, 503-546.
197. Madsen, J.; Armes, S. P.; Lewis, A. L., Preparation and Aqueous Solution Properties of New Thermoresponsive Biocompatible ABA Triblock Copolymer Gelators. *Macromolecules* **2006**, *39*, 7455-7457.
198. Madsen, J.; Armes, S. P.; Bertal, K.; MacNeil, S.; Lewis, A. L., Preparation and Aqueous Solution Properties of Thermoresponsive Biocompatible AB Diblock Copolymers. *Biomacromolecules* **2009**, *10*, 1875-1887.
199. Thompson, K. L.; Williams, M.; Armes, S. P., Colloidosomes: Synthesis, properties and applications. *J. Colloid Interface Sci.* **2015**, *447*, 217-228.
200. Derry, M. J.; Fielding, L. A.; Warren, N. J.; Mable, C. J.; Smith, A. J.; Mykhaylyk, O. O.; Armes, S. P., In situ small-angle X-ray scattering studies of sterically-stabilized diblock copolymer nanoparticles formed during polymerization-induced self-assembly in non-polar media. *Chem. Sci.* **2016**, *7*, 5078-5090.
201. Madivala, B.; Vandebril, S.; Fransaer, J.; Vermant, J., Exploiting particle shape in solid stabilized emulsions. *Soft Matter* **2009**, *5*, 1717-1727.
202. Madivala, B.; Fransaer, J.; Vermant, J., Self-Assembly and Rheology of Ellipsoidal Particles at Interfaces. *Langmuir* **2009**, *25*, 2718-2728.
203. Dugyala, V. R.; Anjali, T. G.; Upendar, S.; Mani, E.; Basavaraj, M. G., Nano ellipsoids at the fluid–fluid interface: effect of surface charge on adsorption, buckling and emulsification. *Faraday Discussions* **2016**, *186*, 419-434.
204. Wang, A.; Rogers, W. B.; Manoharan, V. N., Effects of Contact-Line Pinning on the Adsorption of Nonspherical Colloids at Liquid Interfaces. *Phys Rev Lett* **2017**, *119*, 108004.
205. Loudet, J. C.; Yodh, A. G.; Pouligny, B., Wetting and Contact Lines of Micrometer-Sized Ellipsoids. *Phys Rev Lett* **2006**, *97*, 018304.
206. Xue, Y.; Li, X.; Dong, J., Interfacial characteristics of block copolymer micelles stabilized Pickering emulsion by confocal laser scanning microscopy. *Journal of Colloid and Interface Science* **2020**, *563*, 33-41.
207. Blanazs, A.; Verber, R.; Mykhaylyk, O. O.; Ryan, A. J.; Heath, J. Z.; Douglas, C. W. I.; Armes, S. P., Sterilizable Gels from Thermoresponsive Block Copolymer Worms. *J. Am. Chem. Soc.* **2012**, *134*, 9741-9748.
208. Lovett, J. R.; Ratcliffe, L. P. D.; Warren, N. J.; Armes, S. P.; Smallridge, M. J.; Cracknell, R. B.; Saunders, B. R., A Robust Cross-Linking Strategy for Block Copolymer Worms Prepared via Polymerization-Induced Self-Assembly. *Macromolecules* **2016**, *49*, 2928-2941.
209. Zhang, Q.; Wang, C.; Fu, M.; Wang, J.; Zhu, S., Pickering high internal phase emulsions stabilized by worm-like polymeric nanoaggregates. *Polym. Chem.* **2017**, *8*, 5474-5480.
210. Zhang, Y.; Yu, L.; Dai, X.; Zhang, L.; Tan, J., Structural Difference in Macro-RAFT Agents Redirects Polymerization-Induced Self-Assembly. *ACS Macro Lett.* **2019**, *8*, 1102-1109.
211. Tan, J.; Dai, X.; Zhang, Y.; Yu, L.; Sun, H.; Zhang, L., Photoinitiated Polymerization-Induced Self-Assembly via Visible Light-Induced RAFT-Mediated Emulsion Polymerization. *ACS Macro Lett.* **2019**, *8*, 205-212.

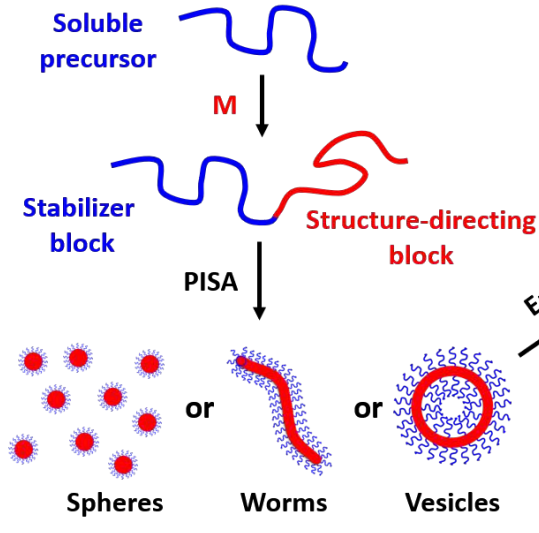
212. Cunningham, V. J.; Armes, S. P.; Musa, O. M., Synthesis, characterisation and Pickering emulsifier performance of poly(stearyl methacrylate)–poly(N-2-(methacryloyloxy)ethyl pyrrolidone) diblock copolymer nano-objects via RAFT dispersion polymerisation in n-dodecane. *Polym. Chem.* **2016**, *7*, 1882-1891.
213. Rymaruk, M. J.; Cunningham, V. J.; Brown, S. L.; Williams, C. N.; Armes, S. P., Oil-in-oil pickering emulsions stabilized by diblock copolymer nanoparticles. *J. Colloid Interface Sci.* **2020**, *580*, 354-364.
214. Shen, L.; Guo, H.; Zheng, J.; Wang, X.; Yang, Y.; An, Z., RAFT Polymerization-Induced Self-Assembly as a Strategy for Versatile Synthesis of Semifluorinated Liquid-Crystalline Block Copolymer Nanoobjects. *ACS Macro Lett.* **2018**, *7*, 287-292.
215. Cai, D.; Thijssen, J. H. T.; Clegg, P. S., Making Non-aqueous High Internal Phase Pickering Emulsions: Influence of Added Polymer and Selective Drying. *ACS Applied Materials & Interfaces* **2014**, *6*, 9214-9219.
216. Pérez-García, M. G.; Carranza, A.; Puig, J. E.; Pojman, J. A.; del Monte, F.; Luna-Bárceñas, G.; Mota-Morales, J. D., Porous monoliths synthesized via polymerization of styrene and divinyl benzene in nonaqueous deep-eutectic solvent-based HIPEs. *RSC Advances* **2015**, *5*, 23255-23260.
217. Rodier, B. J.; de Leon, A.; Hemmingsen, C.; Pentzer, E., Polymerizations in oil-in-oil emulsions using 2D nanoparticle surfactants. *Polym. Chem.* **2018**, *9*, 1547-1550.
218. György, C.; Hunter, S. J.; Girou, C.; Derry, M. J.; Armes, S. P., Synthesis of poly(stearyl methacrylate)-poly(2-hydroxypropyl methacrylate) diblock copolymer nanoparticles via RAFT dispersion polymerization of 2-hydroxypropyl methacrylate in mineral oil. *Polym. Chem.* **2020**, *11*, 4579-4590.
219. Ata, S., Coalescence of Bubbles Covered by Particles. *Langmuir* **2008**, *24*, 6085-6091.
220. Ata, S.; Davis, E. S.; Dupin, D.; Armes, S. P.; Wanless, E. J., Direct Observation of pH-Induced Coalescence of Latex-Stabilized Bubbles Using High-Speed Video Imaging. *Langmuir* **2010**, *26*, 7865-7874.
221. Thompson, K. L.; Giakoumatos, E. C.; Ata, S.; Webber, G. B.; Armes, S. P.; Wanless, E. J., Direct Observation of Giant Pickering Emulsion and Colloidosome Droplet Interaction and Stability. *Langmuir* **2012**, *28*, 16501-16511.
222. Morse, A. J.; Tan, S.-Y.; Giakoumatos, E. C.; Webber, G. B.; Armes, S. P.; Ata, S.; Wanless, E. J., Arrested coalescence behaviour of giant Pickering droplets and colloidosomes stabilised by poly(tert-butylaminoethyl methacrylate) latexes. *Soft Matter* **2014**, *10*, 5669-5681.
223. Ueno, K.; Bournival, G.; Wanless, E. J.; Nakayama, S.; Giakoumatos, E. C.; Nakamura, Y.; Fujii, S., Liquid marble and water droplet interactions and stability. *Soft Matter* **2015**, *11*, 7728-7738.
224. Morse, A. J.; Giakoumatos, E. C.; Tan, S.-Y.; Webber, G. B.; Armes, S. P.; Ata, S.; Wanless, E. J., Giant pH-responsive microgel colloidosomes: preparation, interaction dynamics and stability. *Soft Matter* **2016**, *12*, 1477-1486.
225. Cunningham, V. J.; Giakoumatos, E. C.; Marks, M.; Armes, S. P.; Wanless, E. J., Effect of morphology on interactions between nanoparticle-stabilised air bubbles and oil droplets. *Soft Matter* **2018**, *14*, 3246-3253.
226. Ata, S.; Pugh, R. J.; Jameson, G. J., The influence of interfacial ageing and temperature on the coalescence of oil droplets in water. *Colloids Surf., A* **2011**, *374*, 96-101.
227. Solans, C.; Izquierdo, P.; Nolla, J.; Azemar, N.; Garcia-Celma, M. J., Nano-emulsions. *Curr. Opin. Colloid Interface Sci.* **2005**, *10*, 102-110.
228. McClements, D. J., Nanoemulsions versus microemulsions: terminology, differences, and similarities. *Soft Matter* **2012**, *8*, 1719-1729.
229. Gupta, A.; Eral, H. B.; Hatton, T. A.; Doyle, P. S., Nanoemulsions: formation, properties and applications. *Soft Matter* **2016**, *12*, 2826-2841.
230. Persson, K. H.; Blute, I. A.; Mira, I. C.; Gustafsson, J., Creation of well-defined particle stabilized oil-in-water nanoemulsions. *Colloids Surf., A* **2014**, *459*, 48-57.
231. Sihler, S.; Schrade, A.; Cao, Z.; Ziener, U., Inverse Pickering Emulsions with Droplet Sizes below 500 nm. *Langmuir* **2015**, *31*, 10392-10401.
232. Hunter, S. J.; Penfold, N. J. W.; Chan, D. H.; Mykhaylyk, O. O.; Armes, S. P., How Do Charged End-Groups on the Steric Stabilizer Block Influence the Formation and Long-Term Stability

of Pickering Nanoemulsions Prepared Using Sterically Stabilized Diblock Copolymer Nanoparticles? *Langmuir* **2020**, *36*, 769-780.

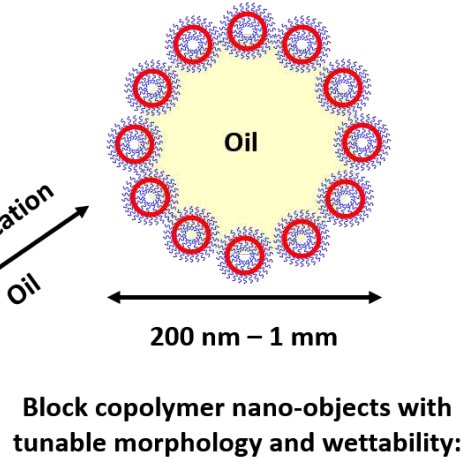
233. Schrade, A.; Landfester, K.; Ziener, U., Pickering-type stabilized nanoparticles by heterophase polymerization. *Chem. Soc. Rev.* **2013**, *42*, 6823-6839.
234. Akpınar, B.; Fielding, L. A.; Cunningham, V. J.; Ning, Y.; Mykhaylyk, O. O.; Fowler, P. W.; Armes, S. P., Determining the Effective Density and Stabilizer Layer Thickness of Sterically Stabilized Nanoparticles. *Macromolecules* **2016**, *49*, 5160-5171.
235. Sun, J.; Erickson, M.; Parr, J., Refractive index matching and clear emulsions. *Journal of cosmetic science* **2005**, *56*, 253-65.
236. Hibberd, D. J.; Mackie, A. R.; Moates, G. K.; Penfold, R.; Watson, A. D.; Barker, G. C., Preparation and characterisation of a novel buoyancy and refractive index matched oil-in-water emulsion. *Colloids Surf., A* **2007**, *301*, 453-461.
237. Husband, F. A.; Garrood, M. J.; Mackie, A. R.; Burnett, G. R.; Wilde, P. J., Adsorbed Protein Secondary and Tertiary Structures by Circular Dichroism and Infrared Spectroscopy with Refractive Index Matched Emulsions. *J Agr Food Chem* **2001**, *49*, 859-866.
238. Cockram, A. A.; Neal, T. J.; Derry, M. J.; Mykhaylyk, O. O.; Williams, N. S. J.; Murray, M. W.; Emmett, S. N.; Armes, S. P., Effect of Monomer Solubility on the Evolution of Copolymer Morphology during Polymerization-Induced Self-Assembly in Aqueous Solution. *Macromolecules* **2017**, *50*, 796-802.
239. Brotherton, E. E.; Hatton, F. L.; Cockram, A. A.; Derry, M. J.; Czajka, A.; Cornel, E. J.; Topham, P. D.; Mykhaylyk, O. O.; Armes, S. P., In Situ Small-Angle X-ray Scattering Studies During Reversible Addition-Fragmentation Chain Transfer Aqueous Emulsion Polymerization. *J. Am. Chem. Soc.* **2019**, *141*, 13664-13675.
240. Hatton, F. L.; Park, A. M.; Zhang, Y.; Fuchs, G. D.; Ober, C. K.; Armes, S. P., Aqueous one-pot synthesis of epoxy-functional diblock copolymer worms from a single monomer: new anisotropic scaffolds for potential charge storage applications. *Polym. Chem.* **2019**, *10*, 194-200.
241. Cornel, E. J.; van Meurs, S.; Smith, T.; O'Hara, P. S.; Armes, S. P., In Situ Spectroscopic Studies of Highly Transparent Nanoparticle Dispersions Enable Assessment of Trithiocarbonate Chain-End Fidelity during RAFT Dispersion Polymerization in Nonpolar Media. *J. Am. Chem. Soc.* **2018**, *140*, 12980-12988.
242. Hunter, S. J.; Cornel, E. J.; Mykhaylyk, O. O.; Armes, S. P., Effect of salt on the formation and stability of water-in-oil Pickering nanoemulsions stabilized by diblock copolymer nanoparticles. *Langmuir* **2020**, *36*, accepted for publication.

# TOC graphic

## Polymerization-induced self-assembly (PISA)



## Pickering emulsion stabilized by block copolymer vesicles



## Author Biographies

**Prof. Steven P. Armes** received his BSc (1983) and PhD (1987) Chemistry degrees from the University of Bristol and worked as a post-doctoral fellow at Los Alamos National Laboratory in New Mexico (1987-89). He accepted a lectureship at Sussex University in 1989 and was promoted to full Professor in 2000. He moved to the University of Sheffield in 2004. He works at the interface of synthetic polymer chemistry and colloid science and has published more than 650 papers to date (H-index 113) His research interests include block copolymer self-assembly, polymerization-induced self-assembly, Pickering emulsions, colloidal nanocomposite particles, microgels, gels, foams, and conducting polymer particles for space science applications.



**Saul J. Hunter** is a current PhD student working in the Armes group at the University of Sheffield. He was awarded the Haworth prize and medal when graduating top of his class with an MChem degree in Chemistry from the same institution in 2017. His EPSRC-sponsored research project is focused on Pickering (nano)emulsions and is partially supported by DSM (The Netherlands). He has co-authored four publications to date, including two papers in *Langmuir*, and he expects to receive his PhD degree by the end of 2021.

